**Title: Newly-discovered Neanderthal remains from Shanidar Cave, Iraqi Kurdistan, and their attribution to Shanidar 5**

**Authors (family names underlined)**

Emma Pomeroy [a]
Marta Mirazón Lahr [b]
Federica Crivellaro [c]
Lucy Farr [d]
Tim Reynolds [e]
Chris O. Hunt [f]
Graeme Barker [g]

**Author affiliations**

[a] School of Natural Sciences and Psychology, Liverpool John Moores University, James Parsons Building, Byrom Street, Liverpool L3 3AF, UK. Email: E.E.Pomeroy@ljmu.ac.uk

[b] Leverhulme Centre for Human Evolutionary Studies, Department of Archaeology and Anthropology, University of Cambridge, Fitzwilliam Street, Cambridge CB2 1QH, UK. Email: mbml1@cam.ac.uk

[c] Leverhulme Centre for Human Evolutionary Studies, Department of Archaeology and Anthropology, University of Cambridge, Fitzwilliam Street, Cambridge CB2 1QH, UK. Email: fc285@cam.ac.uk

[d] McDonald Institute for Archaeological Research, University of Cambridge, Downing Street, Cambridge CB2 3ER, UK. Email: lrf24@cam.ac.uk

[e] Department of History, Classics & Archaeology, Birkbeck College, University of London, Russell Square, London WC1B 5DQ, UK. Email: te.reynolds@bbk.ac.uk

[f] School of Natural Sciences and Psychology, Liverpool John Moores University, James Parsons Building, Byrom Street, Liverpool L3 3AF, UK. Email: C.O.Hunt@ljmu.ac.uk

[g] McDonald Institute for Archaeological Research, University of Cambridge, Downing Street, Cambridge CB2 3ER, UK. Email: gb314@cam.ac.uk

**Corresponding author**

Dr Emma Pomeroy
School of Natural Sciences and Psychology
Liverpool John Moores University
James Parsons Building
Byrom Street
Liverpool L3 3AF
UK

Tel: (+44) 151 231 2815
Email: E.E.Pomeroy@ljmu.ac.uk

**Abstract**

The Neanderthal remains from Shanidar Cave, excavated between 1951 and 1960, have played a central role in debates concerning diverse aspects of Neanderthal morphology and behavior. In 2015 and 2016, renewed excavations at the site uncovered hominin remains from the immediate area where the partial skeleton of Shanidar 5 was found in 1960. Shanidar 5 was a robust adult male estimated to have been aged over 40 years at the time of death. Comparisons of photographs from the previous and recent excavations indicate that the old and new remains were directly adjacent to one another, while the disturbed arrangement and partial crushing of the new fossils is consistent with descriptions and photographs of the older discoveries. The newly-discovered bones include fragments of several vertebrae, a left hamate, part of the proximal left femur and a heavily crushed partial pelvis, and the distal half of the right tibia and fibula and associated talus and navicular. All these elements were previously missing from Shanidar 5, and morphological and metric data are consistent with the new elements belonging to this individual. A newly-discovered partial left pubic symphysis indicates an age at death of 40–50 years, also consistent with the age of Shanidar 5 estimated previously. Thus the combined evidence strongly suggests that the new finds can be attributed to Shanidar 5. Ongoing analyses of associated samples, including for sediment morphology, palynology, and dating, will therefore offer new evidence as to how this individual was deposited in the cave, and permit new analyses of the skeleton itself and broader discussion of Neanderthal morphology and variation.

**Keywords:** hominin skeletal remains; postcrania; hand; foot; morphology

## 1. Introduction

Excavations led by Ralph Solecki from 1951 to 1960 at Shanidar Cave in the Zagros Mountains, Iraqi Kurdistan (Fig. 1A-B; Supplementary Online Material [SOM] Fig. S1), yielded the remains of 10 Neanderthal individuals (Solecki, 1961, 1963, 1971; Trinkaus, 1983b; Cowgill et al., 2007). The skeletons vary in their degree of completeness, but range in age from infants to older adults at the time of death and represent both males and females (Trinkaus, 1983b; Cowgill et al., 2007). The Shanidar Neanderthals have played a key role in debates regarding Neanderthal biology and behavior, including social behaviors such as care for the ill and injured (Dettwyler, 1991; Trinkaus, 1983b), mortuary practices (Leroi-Gourhan, 1975; Solecki, 1975; Gargett, 1999; Sommer, 1999), interpersonal violence (Stewart, 1969; Trinkaus and Zimmerman, 1982; Trinkaus, 1983b; Churchill et al., 2009), and artificial cranial modification (Trinkaus, 1982; Chech et al., 1999; Clark et al., 2007); aspects of growth (Martín-González et al., 2012), health (Trinkaus, 1983b; Crubézy and Trinkaus, 1992; Berger and Trinkaus, 1995; Anton, 1997 ), diet (Henry et al., 2011) and demography (Trinkaus and Thompson, 1987); as well as morphological variation and its causes (Trinkaus, 1981, 1983b; Pearson, 2000; Pablos et al. 2017a).

[FIGURE 1 NEAR HERE]

Solecki (1961, 1963, 1971) ascribed the original burials to two main periods within his 'Layer D' (Fig. 1C). Shanidar 1, 3 and 5 were assigned to around 46–50 ka based on radiocarbon dates from charcoal associated with Shanidar 1 (Solecki, 1971). Although this date needs to be regarded cautiously, more recent redating of the site has broadly supported this chronology (Cowgill et al., 2007). The remaining burials exposed during Solecki's excavation, Shanidar 2, 4, 6, 7, 8, 9 and 10, were assigned to an earlier period estimated to be between 60 and 100 ka (Solecki, 1971; Cowgill et al., 2007), although these are inferred rather than direct dates and should therefore be taken as tentative (Cowgill et al., 2007).

### *1.1. The Shanidar 5 individual*

Shanidar 5 was originally discovered by Ralph Solecki, who excavated the skeleton with T. Dale Stewart in August 1960 (Solecki, 1961). The fragmented remains of this individual were found at a depth of 4.39–4.48 m below Solecki's datum, at the top of his 'Layer D' (Solecki, 1961; Trinkaus, 1977; Figs. 1B and 2A). Therefore, along with Shanidar 1 and 3, Shanidar 5 was one of the stratigraphically most recent Neanderthal individuals discovered at the cave, and Solecki considered Shanidar 1 and 5 to have been contemporaneous. Analysis of charcoal recovered close to Shanidar 1 gave radiocarbon dates of ca. 46–50 ka (Solecki, 1961, 1971).

[FIGURE 2 NEAR HERE]

The remains of Shanidar 5 were "badly damaged and scattered" (Trinkaus, 1977: 34), with many of the bones found beneath or between rocks, and with evidence of additional disturbance by rodent activity. On the basis of its position, Shanidar 5 was interpreted as the victim of a rock fall (Solecki, 1961; 1971; Stewart, 1977; Trinkaus, 1983b). The pelvis was found crushed below a large rock, on top of which lay the cranium. This large rock was thought to have fallen onto the individual's back, pushing the body face down and forcing the head back so that it came to lie above the rock (Trinkaus, 1983b: 27), while the lower limb bones lay partially under other smaller rocks (Stewart, 1977: Fig. 2). The skeleton was generally very fragmented, and the lower limb bones were friable in places. The lower limbs were flexed and lying on their anterior surfaces in approximate articulation but demonstrating some disturbance (Solecki, 1971; Stewart, 1977; Trinkaus, 1977, 1983b). Some remains of the upper limbs and torso were also recovered "out of context" (Trinkaus, 1983b: 27). The cranium and pelvis were removed along with the large stone, while the limb bones were recovered separately. All the remains were first unpacked and studied by Erik Trinkaus in 1976 (Trinkaus, 1977, 1983b) at the Iraq Museum, Baghdad, where they have been curated since their excavation.

Trinkaus (1977, 1983b, 1987) identified Shanidar 5 as a male, aged 40 years or more at death (based on femoral histomorphology and supported by dental wear), and noted the individual's exceptionally large and robust cranium (Trinkaus, 1982, 1983b). Although a number of the major bones were at least partially recovered, the skeleton was incomplete, and missing in particular were the mandible and most of the dentition, much of the vertebral column, both humeri, the left radius, the right tibia and fibula, parts of

both hands and the whole of both feet (Trinkaus, 1983b). The combination of the large overburden that lay above parts of Shanidar 5 and the timing of the discovery of the skeleton within days of Shanidar 4, 6, 8 and 9 at the end of the last season of excavation at the site, meant that the material was not fully recovered. Indeed, Trinkaus (1977: 34) stated that "portions of Shanidar 5 were left in situ" and that future excavations might well unearth more of the skeleton.

*1.2. New investigations at Shanidar Cave*

In 2014, new excavations began at Shanidar Cave at the invitation of the Kurdish Regional Government. The aim is to establish a high resolution chronological, cultural, sedimentological and paleoenvironmental framework for the Paleolithic occupations and to re-investigate the chronology, nature, and origin (anthropogenic vs. natural) of the Neanderthal remains by revisiting Solecki's trench and conducting new targeted investigations within and adjacent to it (Fig. 1D,E; SOM Fig. S1; Reynolds et al., 2015, 2016).

During the 2015 and 2016 seasons, section cleaning and new excavations at the edge of Solecki's trench, in the vicinity of the Shanidar 5 find-spot, yielded new hominin remains (Reynolds et al., 2015, 2016). This paper presents the first description of these remains, and attempts to answer two specific questions. The first is whether the material can be confidently identified as Neanderthal. The precise location of the new finds make it very likely that these are Neanderthal remains, but the presence of modern humans in the broader southwest Asian region from around 100 ka onwards (McCown and Keith, 1939; McDermott et al., 1993) makes it important to confirm the taxonomic affinity of every set or remains found in this area, particularly given the close proximity of the remains we describe here to presumed Upper Paleolithic (Baradostian) levels at the site. The second is whether the remains are likely to represent a single individual, and in particular Shanidar 5. The identification of the new material as belonging to this previously incomplete skeleton would offer a direct link between the two excavations and the novel information arising from the detailed modern studies which are currently underway, including dating, stratigraphic, sedimentological, paleontological and artifactual analyses.

## 2. Materials and methods

During the course of excavations in 2015, a partial, fragmented lower right hominin leg and part of the associated right foot preserving a complete talus and navicular were discovered, all in approximate articulation with one another (Fig. 3). This find was followed by that of the left hip region (partial pelvis and proximal left femur) in spring 2016 (Fig. 4), which was directly adjacent to the 2015 finds and tight against the base of a medium-sized stone. The pelvic remains included a partial pubic symphysis, which can offer evidence on age at death. Other bones from the left hand, right and left feet and trunk were also discovered, which are described below. Preservation of the remains is very variable. In general, the bones are crushed and highly fragmented. Some elements, such as the talus and navicular, are well preserved, whereas others, such as the pelvis and proximal part of the femur, were fragile and friable. There is evidence of disturbance by rodent burrowing, particularly in the case of the right foot (Fig. 3).

[FIGURE 3 NEAR HERE]

[FIGURE 4 NEAR HERE]

Comparison of our excavations with published photographs from those carried out by Solecki provides a strong indication that the new remains are from Shanidar 5. A rock beside the left hip remains discovered in 2016 can be confidently identified in a published image of the Shanidar 5 limbs during excavation in 1960 (Fig. 2), and so demonstrates fairly conclusively that the left hip remains lay directly below and adjacent to the lower limb bones recovered at the time. In addition, although the photographs are not from precisely the same angle, the left femoral shaft visible in Solecki's photograph aligns almost perfectly with the more proximal section of left femoral shaft recovered in 2016. Nonetheless it remains important to examine additional evidence that might link the old and new finds, including comparisons of morphology and dimensions with published data on Shanidar 5, other Neanderthals and modern humans, and confirmation that no elements are duplicated, in order to further demonstrate that we are dealing with a single individual.

The new remains were loaned for study to the McDonald Institute of Archaeological Research at the University of Cambridge, UK, with the kind permission of the Kurdistan General Directorate of Antiquities,

and will be returned to the Directorate following study for long term curation. The new remains were measured using digital sliding callipers (Mitutoyo Inc., Japan) to the nearest 0.1 mm, or coordinate callipers (GPM, Switzerland) to the nearest 1 mm where appropriate. Sources for measurement definitions vary by element, and are referenced in the relevant tables. In the comparison of the left hamate with published measurements from the Shanidar 3 and 5 right hamates, to assess whether the new bone may pertain to one of these individuals, bilateral asymmetry was calculated as the absolute difference between measurements of right and left bones (see also SOM).

Age at death was estimated using pubic symphyseal morphology following both the Todd and Suchey-Brooks methods (Todd, 1920, 1921; Brooks and Suchey, 1990) in accordance with current recommendations (Buikstra and Ubelaker, 1994; White et al., 2011). Any age estimates must be treated with caution, as the standards commonly applied are based on recent modern human populations and their reliability even in recent populations can be problematic (e.g., Molleson and Cox, 1993; Schmitt et al., 2002), while their applicability to early *Homo sapiens*, let alone to other hominins such as Neanderthals (Trinkaus, 1983b), is unknown. Degeneration of the joint surfaces might be accelerated by elevated activity levels (Mays, 2015), which is often inferred for Neanderthals given skeletal evidence for high levels of biomechanical loading (Trinkaus, 1983a, 1983b; Ruff et al., 1993; Trinkaus and Rhoads, 1999; Pearson et al., 2006; Weaver, 2009) and which might lead to an overestimate of an individual's true age at death.

To give new insights into body size, stature was estimated from the total talus length (Martin number 1a) using the equation derived from Euroamerican males (Pablos et al., 2013a), and using equations derived from various talar measurements (Will and Stock 2015). Body mass was also estimated using equations for talar measurements through two different methods, one that estimates body mass directly (McHenry, 1992) and another that uses talar dimensions to estimate femoral head diameter (Will and Stock, 2015) which, in turn, is used to estimate body mass. To estimate body mass from femoral head diameter, the mean estimate generated by the equations of Ruff et al. (1991), McHenry (1992) and Grine et al. (1995) was used for femoral head diameters ≤ 47 mm, and the mean of Ruff et al. (1991) and Grine et al. (1995) was used for femoral head diameters > 47 mm, following Will and Stock (2015) and Ruff (2010). Pooled sex equations were used in all cases following Plavcan et al. (2014).

It should be noted that the approaches for stature and body mass estimation suffer from multiple problems. The equations are derived from recent samples of *H. sapiens*, which may differ from other hominin species in the relationships between body size and skeletal dimensions. It is widely acknowledged that variation in limb and trunk proportions in relation to climate and other factors reduce the reliability of applying equations derived from one population to skeletons from another, even within species (e.g., Pearson, 1899; Trotter and Gleser, 1952; Trotter, 1970; Holliday and Ruff, 1997; Auerbach and Ruff, 2008; Pomeroy and Stock, 2012; Ruff et al., 2012). In addition, the long bones of the limbs, especially the lower limbs, are the preferred individual elements for stature estimation and provide the most reliable results (e.g., Pablos et al., 2013a; Will and Stock, 2015), presumably because those bones make a substantial contribution to an individual's actual stature. Furthermore, the method of Will and Stock (2015) involves multiple estimates (femoral head diameter from talar dimensions, then body mass from femoral head diameter). Errors will be introduced at each step of estimation, potentially limiting the reliability of results (Feldesman and Lundy, 1988; Porter, 2002; Will and Stock, 2015). Sample sizes from which the equations were derived were small (n = 18–19), which may also limit their reliability. Therefore the estimates generated here should be treated with extreme caution, although are presented since they potentially offer additional new data on body size variation among Neanderthals and insights into the reliability of methods developed from (largely recent) *H. sapiens* skeletons when applied to hominin species such as Neanderthals.

## 3. Results

The new skeletal remains recovered from the area around the original Shanidar 5 skeleton are listed in Table 1, followed by descriptions of the individual specimens by anatomical region and a discussion of estimated age at death, body size estimates and pathological changes to the skeleton. Larger and more complete bones or fragments are illustrated in the text, while the remaining elements are illustrated in SOM Fig. S2 (see Table 1 for details).

[TABLE 1 NEAR HERE]

*3.1. Axial skeleton*

3.1.1. Vertebrae Three vertebral fragments and a piece of the sacrum were found in the region around the tibia, fibula and tarsals.

A left superior facet of a probable upper cervical vertebra (SH15A 72.2: SOM Fig. S2) was found in two refitting pieces, including the base of the transverse process and lateral margin of the transverse foramen. Following Gómez-Olivencia et al. (2013a) the sagittal and transverse diameters of the facet are 15.0 mm and 12.2 mm respectively.

SH15A 72.1 is the complete spinous process of a probable mid-thoracic vertebra, identified on the basis of its size, narrow mediolateral dimensions, and lack of bifurcation (SOM Fig. S2). Following Gómez-Olivencia et al. (2013a), the transverse diameter of the spinous process tip is 3.1 mm, and the minimum transverse diameter of the spinous process is 5.5 mm.

An 18 mm by 14 mm section of the margin of a vertebral body (SH15A 64.1: SOM Fig. S2) is tentatively identified as thoracic on the basis of size. The annular epiphysis is fully fused and there is no sign of any degenerative changes.

An almost complete adult thoracic vertebral body (SH16 269: Fig. 5) was recovered from the region of the left proximal femur and pelvis. The preserved portion includes part of the left pedicle, but the right pedicle is missing and there is minor damage to the lateral aspect of the body on the right side. Based on size (Table 2) and shape, this vertebra is from the mid-upper thoracic region, as its dimensions fall between Neanderthal second and seventh thoracic vertebrae as given by Gómez-Olivencia et al. (2013b). The annular epiphyses are both well fused, indicating an adult individual. The left superior costal demifacet is almost imperceptible, but the corresponding inferior demifacet is more clearly visible, while on the right the demifacet is missing superiorly and is visible, but very small inferiorly. There is a slight anterior extension to the inferior surface of the body projecting approximately 1.8 mm from the normal margin of the body representing mild degenerative changes (see subsection 3.6 below). While the vertebrae, and especially the thoracic vertebrae, are commonly thought to be of limited value in assessing taxonomic

affinities, recent work indicates that the Neanderthal thoracic spine does show some unique characters (Gómez-Olivencia et al., 2013b; Bastir et al. 2017). However, without confidently identifying the anatomical location of the vertebra, these criteria cannot be applied here.

[FIGURE 5 NEAR HERE]

SH15A 64.4 is a small fragment of the posterosuperior aspect of the left sacroiliac joint of the sacrum, which includes part of the posterior surface of the sacrum (SOM Fig. S2). The whole fragment measures 21 mm by 23 mm.

[TABLE 2 NEAR HERE]

3.1.2. Pelvis An area of highly fragile and extensively crushed pelvic remains was found in 2016 in association with the remains of the proximal left femur, tight against the west side of the rock identified in Figure 2. Nonetheless, a number of identifiable fragments were recovered including the left pubic symphysis (SH16 239.1) and left superior pubic ramus (SH16 239.2), which are informative on age at death and taxonomy respectively. The original remains of Shanidar 5 included only fragments of the iliac blades that could not be assigned to a specific side of the body (Trinkaus, 1983b), limiting the possibility of matching the new remains to the existing ones. Portions of the ilia were also discovered during the 2016 excavations (SH16 278), but as with those found in 1960, these are too fragmented to be informative. However, it is notable that all of the identifiable new pelvic remains in which side could be determined were from the left side of the body.

The pubic symphysis (SH16 239.1) comprises six refitting fragments, and while incomplete, preserves a substantial part of the inferior half of the pubic symphysis, including the inferior extremity, around 65% of the dorsal margin, and a small section of the ventral margin (Fig. 6). The small preserved section of inferior pubic ramus suggests a relatively wide subpubic angle characteristic of Neanderthals and modern human females (Trinkaus, 1983b; Rak, 1990), although it is insufficiently preserved to allow an estimated measurement of the angle.

[FIGURE 6 NEAR HERE]

SH16 239.2 is a partial left superior pubic ramus measuring 35 mm in length and comprised of 3 fragments (SOM Fig. S2). In common with some other Neanderthal specimens, it has a clearly developed,

flat and blade-like (but damaged) crest along the superior edge (McCown and Keith, 1939; Stewart, 1960; Trinkaus, 1976, 1983b; Rak and Arensburg, 1987). Other identifiable fragments include a more lateral fragment of the pubis (SH16 245.3: SOM Fig. S2) and unsided fragments of the obturator foramen (SH16 239.3 and 245.4: SOM Fig. S2). All the pelvic remains described thus far were recovered from the region where the proximal femur was found, but at least one fragment was also recovered from the region around the tibia, fibula and tarsals: SH15A 65 is a fragment of the visceral surface of the left greater sciatic notch, measuring approximately 30 x 30 mm (SOM Fig. S2). It is insufficiently preserved to permit sex estimation, but includes the very edge of the left auricular surface and part of the arcuate line.

*3.2. Upper limb*

Two carpals, the left hamate and a fragment of left trapezoid are the only remains from the upper limbs uncovered by the new excavations.

3.2.1. Hamate The adult left hamate was retrieved in the spring 2015 field season from an unstratified context in the vicinity of the original Shanidar 5 finds, before the rest of the material reported here was discovered. The hamate is one of the more distinctive bones of the Neanderthal wrist, having an absolutely and relatively large and robust hamulus (Trinkaus, 1983b; Niewoehner et al., 1997). Together with the fact that the right (but not left) hamates of Shanidar 3 and Shanidar 5 were recovered in previous excavations, this offers the possibility of attributing the left hamate to one (or neither) of these individuals and further testing the Neanderthal affinity of the remains. Shanidar 3 was found close to, but deeper than, Shanidar 5 and so merits consideration here given the unstratified nature of the new hamate.

SH15 590 is broken into two refitting fragments that preserve most of the body and the entire hamulus (Fig. 7). There is a portion of the dorsal surface of the body missing, including the dorsolateral aspect of the fifth metacarpal articular facet and the distal portion of the capitate facet. Visually, the hamate demonstrates the long, thick and projecting hamulus and relatively short body characteristic of Neanderthals, which is confirmed by metric data (Table 3, Fig. 8). While there is overlap between Neanderthal and *H. sapiens* morphology, the most diagnostic measurements for distinguishing between

published data on Neanderthals, Late Pleistocene *H. sapiens* and a broad geographic sample of recent *H. sapiens* (see Table 3 and SOM) include hamulus length and hamulus projection index (hamulus projection relative to maximum height). Bivariate plots of articular length and hamulus projection index against hamulus length show that SH15 590 plots with Neanderthals rather than *H. sapiens* (Fig. 8).

[FIGURE 7 NEAR HERE]

[FIGURE 8 NEAR HERE]

[TABLE 3 NEAR HERE]

In order to assess whether the left hamate could plausibly belong to either of the previous individuals preserving the right hamate and found in the vicinity (Shanidar 3 or 5), the degree of bilateral asymmetry was calculated for paired right and left bones from a range of recent *H. sapiens*, and the results compared to the differences between each of the Shanidar 3 and 5 right hamates and the SH15 590 left hamate (SOM Text S1 and Tables S1 and S2). The results indicate that SH15 590 could plausibly be attributed to Shanidar 5, but not to Shanidar 3. Excluding the maximum height measurement, which was estimated due to the fragment missing from SH15 590, the mean difference in measurements between SH15 590 and the Shanidar 3 right hamate was 2.0 mm, approximately 3 times greater than that observed in the modern human sample, and considerably larger than the mean difference between SH15 590 and the Shanidar 5 right hamate (0.3 mm). This mean difference falls within the range for the difference between right and left hamate bones in the comparative sample of *H. sapiens* (0.2–0.7 mm), indicating that the size of SH15 590 is consistent with it belonging to Shanidar 5. The SH15 590 left hamate is shown compared to the Shanidar 5 right hamate in SOM Figure S3.

3.2.2 Other hand remains A small fragment of the left trapezoid (SH15A 64.3: SOM Fig. S2) preserves partial facets for the capitate, scaphoid, and the medial portion of the second metacarpal. It is extensively damaged and covered by a hard, whitish concretion (similar to the tibia and fibula remains) on approximately 50% of its surface.

*3.3. Lower limb*

3.3.1. Femur The proximal left femur was found in association with, and partly overlain by, parts of the left side of the pelvis (Fig. 4). The elements were lying with their anterior surfaces down and posterior surfaces facing upward (as with the original Shanidar 5 finds; Trinkaus 1977, 1983b). Much of the femoral head, trochanter and pelvic remains were extensively crushed and highly fragile.

A ~50 mm long fragment of the posterior half of the proximal left femoral shaft (i.e., the subtrochanteric region) was relatively well preserved and was retrieved in seven refitting fragments (SH16 238: Fig. 9). The very base of the lesser trochanter, as well as sections of the spiral line, pectineal line, linea aspera and gluteal tuberosity are identifiable. The preserved area of gluteal tuberosity is rugged but insufficiently preserved to allow comparative measurements of the midtuberosity breadth or to assess the presence of a hypotrochanteric fossa (cf. Trinkaus 1983b). The cortex of the bone is 8.7 mm thick in the region just distal to the root of the spiral line.

[FIGURE 9 NEAR HERE]

A fragment of the posterolateral part of the lower edge of the left greater trochanter (SH16 271.1: SOM Fig. S2), measuring approximately 40 x 20 mm, was also identified. Other fragments of the greater trochanter and small fragments of the femoral neck (SH16 245.1: SOM Fig. S2) and head (SH16 245.2: SOM Fig. S2) could be identified, although none of the remains were sufficiently intact to permit extensive metric or morphological analysis, or to allow an independent attribution to the left or right side of the body.

3.3.2. Tibia and fibula Substantial portions of the distal half of an adult right tibia and fibula were found lying on their medial side and approximately in articulation with one another and with the talus and navicular, although some movement from original anatomical position was evident (Fig. 3). The bones lay on a 45º slope, with the tarsals lying at the highest point (Reynolds et al., 2015, 2016). A burrow had disturbed the rest of the foot (Fig. 3; Reynolds et al., 2015). Both the tibia and fibula were variably preserved and very fragmented, and the proximal ends of both bones and the distal end of the fibula were entirely missing. This severely limits any metric and morphological analyses of the remains. In both cases, the tibial and fibular shafts have a relatively thick cortex and heavily striated external cortical surface. Both the tibial and fibular fragments are covered by a patchy thin layer of a hard, whitish deposit that

particularly affects the distal tibia and invades the trabecular bone along the lines of long-standing breaks (Fig. 9).

The distal epiphysis of the right tibia is largely complete, although missing the medial malleolus. The talar facet is broken diagonally into two refitting fragments, although some damage has occurred to the broken edges. Nonetheless the refit between fragments is sufficiently tight to permit a reliable measurement of the distal lateral articular breadth, which is 29.3 mm. While a substantial part of the Shanidar 5 left tibia was recovered previously (Trinkaus, 1977, 1983b), this did not include the antimere of the distal articular surface we describe here. Nevertheless, the distal lateral articular breadth of SH15A 64.12 is intermediate between those recorded for Shanidar 1 (33.0 mm) and Shanidar 2 (28.6 mm; Trinkaus, 1983b), thus within the size range of the larger of the Shanidar Neanderthal remains. The posterior border of the joint surface shows slight lipping along most of its length indicative of mild osteoarthritic changes (Rogers and Waldron, 1995).

The SH15A 64.12 distal right tibia displays a lateral ankle flexion (or 'squatting') facet (Fig. 9) measuring 14.9 mm by 4.5 mm at its greatest extent. Ankle flexion facets are extensions of the distal tibial and/or talar articular surfaces due to habitual hyperdorsiflexion of the ankle joint (Trinkaus, 1975b; Capasso et al., 1999). These lateral facet extensions on the distal tibia are common among Neanderthals, affecting 83% of European and southwest Asian individuals studied by Trinkaus (1975b), and are observed on the tibiae of Shanidar 1 and 3 (although not Shanidar 2; Trinkaus, 1983b). These facets are often considered to indicate habitual squatting behaviour, although other causes have also been postulated such as locomotor stresses associated with travelling over uneven or steep terrain (Trinkaus, 1975b; Capasso et al., 1999).

3.3.3 Talus A small portion of an adult left talus (SH15A 64.5 and 76.1: SOM Fig. S2) and a complete right talus (SH15A 69.1: Fig. 10) were recovered. The left talus is represented only by two small refitting fragments of the medial posterior process and the posterior-most margin of the posterior subtalar facet. While these fragments are too small to be measured or extensively described, their morphology matches the right bone very closely (SOM Fig. S4), suggesting that they belong to one individual.

The complete right talus (SH15A 69.1) was found in articulation with the right navicular. It demonstrates an old postmortem transverse break across the neck region, but the fragments refit closely (Fig. 10). While there is some minor erosion to the margins of the joint surfaces, the talus is in extremely good condition.

[FIGURE 10 NEAR HERE]

Many characteristics of Neanderthal tali fall within the modern human range, albeit tending to have larger joint surfaces and to fall at the more robust end of the distribution (Rhoads and Trinkaus, 1977; Trinkaus, 1983b; Mersey et al., 2013; Pablos et al., 2013b, 2017a). The morphology of SH15A 69.1 is consistent with this pattern. Characteristics previously identified as distinguishing Neanderthal tali from those of *H. sapiens* include a short head and neck relative to the trochlea, a mediolaterally wide head, a broad lateral malleolar facet, a short medial subtalar facet, and a square trochlea (Rhoads and Trinkaus, 1977; Trinkaus, 1983a, 1983b; Pablos et al., 2013b, 2017a).

Comparisons of measurements from SH15A 69.1 with published data (Table 4) indicate that it shares a short neck and head relative to the trochlea with published Neanderthal specimens (Trinkaus, 1975a, 1983a, 1983b; Rhoads and Trinkaus, 1977; Pablos et al., 2013b), with a head-neck length/trochlear length ratio closer to the Neanderthal than Late Pleistocene or recent modern human means, but is still within the modern human range. The head is mediolaterally broad, consistent with the Neanderthal mean but greater than the modern human mean, although again there is overlap between the species. The lateral malleolar facet is not particularly broad, although again there is considerable overlap between *H. sapiens* and Neanderthals in this characteristic. SH15A 69.1 also shows a short medial subtalar facet compared with the modern human mean, but comparable with the Neanderthal mean (Table 4).

The talus also shows other morphological characteristics more common in Neanderthals than *H. sapiens*. The trochlea is square rather than posteriorly narrow and the anterior and middle calcaneal articular surfaces are completely fused. This fusion of the facets is seen in 96% of Neanderthals (n = 25; data from Trinkaus, 1975a; Mersey et al., 2013; Pablos et al., 2012) and all 17 specimens from Sima de los Huesos (Pablos et al., 2012, 2013b). This compares with 88.9% of Pleistocene *H. sapiens* (n = 17) and 55–75% of individuals in samples of recent *H. sapiens* (Trinkaus, 1975a: Table 64; Pablos et al., 2012). Finally, there is an anterior extension of both the medial malleolar and medial trochlear articular surfaces. The

former is found in all Neanderthal individuals (n=19) and 52–100% of individuals in recent modern human samples, while the latter characterises 47.2% of Neanderthals (n=18) and 42–100% of individuals in recent modern human samples (Trinkaus, 1975a, b).

Similar to the distal tibia and navicular articular surfaces, there is slight lipping around the margin of the posterior calcaneal facet and the inferior edges of the medial and lateral facets, consistent with mild joint degeneration. However, there is no lateral ankle flexion facet on the superior talar surface to correspond with that of the distal tibia.

[TABLE 4 NEAR HERE]

3.3.4. Navicular SH15A 69.2 is a complete adult right navicular found in articulation with the right talus (SH15A 69.1). It is extremely well preserved, with only minor damage to the margins of the articular surfaces (Fig. 10). The navicular demonstrates clear Neanderthal affinities: it is broad, with a markedly expanded tuberosity for the attachment of the plantar calcaneo-navicular ligament and the insertion of the tibialis posterior muscle. This expanded tuberosity is commonly observed in other Neanderthal specimens (McCown and Keith, 1939; Heim, 1982; Trinkaus, 1983b; Harvati et al., 2013; Mersey et al., 2013) and to a lesser extent in the earlier Sima de los Huesos hominins (Pablos et al., 2007), but distinct from *H. sapiens*. Even the earliest relatively complete modern humans (*H. sapiens*), from Skhul and Qafzeh in southwest Asia, lack a pronounced tuberosity (McCown and Keith, 1939; Vandermeersch, 1981). The expanded tuberosity is thought to indicate reinforcement of the medial longitudinal arch as a response to greater overall loading and consequent robustness of the Neanderthal lower limb skeleton (Rhoads and Trinkaus, 1977; Vandermeersch, 1981; Trinkaus, 1983a, 1983b). In common with other Neanderthal navicular bones (Heim, 1982; Mersey et al., 2013), there is no groove between the talar facet and the tuberosity, reflecting expansion of the latter. The lateral cuneiform facet is deep and concave, the medial cuneiform facet is well defined and relatively triangular in shape, and the talar facet is subrectangular. Slight lipping of the margin of the talar articular surface is present inferomedially and superolaterally.

Measurements of the SH15A 69.2 navicular (Table 5) confirm the expansion of the tuberosity and the Neanderthal affinities of this specimen. Neanderthals are characterized by similar levels of thickness at the medial and lateral cuneiform facets of the navicular compared with modern humans, as reflected by the

wedging index, and high maximum thickness relative to the minimum thickness compared with modern humans. As illustrated in Figure 11, SH15A 69.2 falls clearly within the Neanderthal range, and is outside of the *H. sapiens* range of variation, for both the wedging index and the relationship between maximum and minimum thickness. Similarly, the thickness of the tuberosity relative to the minimum (i.e., lateral) thickness of the navicular (tuberosity thickness index) is at the upper end of the Neanderthal range, more than 2 standard deviations above the mean of a recent Native American sample, and much larger than the remains of early *H. sapiens* from Skhul 4 (Table 5). SH15A 69.2 has a low wedging index compared to a modern human sample given by Harvati et al. (2013) and the values for individuals of early *H. sapiens*, including Skhul 4 (44.8; McCown and Keith, 1939) and Omo 1 (49.2; Pearson et al., 2008), but within the range of published Neanderthal specimens (Table 5).

[FIGURE 11 NEAR HERE]

[TABLE 5 NEAR HERE]

3.3.5. Other tarsals Other tarsal bones recovered are partial and highly fragmentary, precluding any detailed comparative analyses. Identifiable fragments include a small fragment of the right calcaneus (lateral edge of the calcaneal tuberosity: SH15A 64.16: SOM Fig. S2), the dorsal half of the left intermediate cuneiform (SH15A 64.2: SOM Fig. S2), and a small fragment of left lateral cuneiform (partial navicular/intermediate cuneiform facet: SH15A 64.10: SOM Fig. S2). A limited suite of measurements could be collected from the intermediate cuneiform (Table 6), and comparisons with published data on the Sima de los Huesos hominins, other Neanderthals, Late Pleistocene and recent *H. sapiens* indicate that SH15A 64.10 falls within the range of all of these groups.

[TABLE 6 NEAR HERE]

3.3.6. Metatarsals The metatarsals are similarly represented only by fragments that are insufficiently preserved to allow detailed comparative analyses. A fragment of the base of the fifth left metatarsal (SH15A 64.8: SOM Fig. S2) and a metatarsal head (possibly second or third left, based on the size and orientation of the head: SH15A 64.9: SOM Fig. S2) were identified. Measurements were only possible on the metatarsal head (SH15A 64.9) and are given in Table 7. There is considerable overlap between recent *H. sapiens* and Neanderthals in these measurements (Pablos et al., 2012: Table 4).

[TABLE 7 NEAR HERE]

3.3.7. Pedal phalanx A single distal toe phalanx (SH16A 591) was recovered in September 2016 from the same area as the other remains described in this paper (Fig. 12). It is included here on the grounds that it most likely pertains to the same individual, although this cannot be confirmed morphologically due to a lack of other similar bones. It is likely a distal phalanx of the second toe (DP-2) based on size and morphology, although it is large compared with material of recent *H. sapiens*. It is relatively short and wide and lacks lateral deviation of the distal tuberosity relative to the orientation of the proximal facet, so it is unlikely to be a first phalanx. Comparison with measurements for other Shanidar distal phalanges suggests it is from the second or third toe, and most probably the second given its size (Table 8). Neanderthal manual and pedal phalanges are generally larger than those of more recent *H. sapiens* (Trinkaus, 1975a, 1983b), and assuming SH16A 591 is a second or third distal phalanx, its distal breadth of 10.4 mm falls outside the range of Trinkaus' (1983b) Holocene Native American sample for distal breadth (DP-2: 7.5 ± 0.8 mm, n = 14; DP-3: 7.0 ± 1.1 mm, n = 16; DP-4: 6.4 ± 0.7 mm, n = 11; DP-5: 5.2 ± 1.1 mm, n = 20). However, it is similar to the mean of other Neanderthal second and third distal pedal phalanges (10.0 ± 1.3 mm, n = 10; data from Trinkaus, 1975a, 1983b). This specimen is therefore most consistently identified as a Neanderthal phalanx. The proximal articular facet is shallow and the division of the facet into medial and lateral parts is barely discernible. There is osteophyte formation around the proximal joint surface, which is particularly marked medially and laterally (Fig. 12).

[FIGURE 12 NEAR HERE]

[TABLE 8 NEAR HERE]

*3.4. Estimated age at death*

All visible epiphyses of the new remains are fully fused, indicating adult status. The partial left pubic symphysis (SH16 239.1) permits a more precise estimate of age at death. SH16 239.1 shows strong dorsal lipping, with extension to the margin of the pubic symphysis of up to 5 mm dorsally by a large, continuous osteophytic outgrowth separated from the original surface by a deep porous cavity (Fig. 6). The surface of

the pubic symphysis has a faint hint of transverse ridges and furrows remaining, and there is no clear rim to the face in its inferior extremity, although a rim is forming across the dorsal border. This combination of characteristics means that the symphysis does not obviously match a single stage of the Todd or Suchey-Brooks methods. Using Todd (1920, 1921), the following characteristics suggest phase 9 (age 40–45 years): the defined inferior extremity; porosity of the symphyseal face but retention of faint ridges; incomplete symphyseal rim suggested by a hiatus at the limit of the preserved ventral section; and marked dorsal lipping along the preserved length of the dorsal margin but a lack of lipping on the (admittedly incomplete) ventral margin. By the Suchey-Brooks method (Brooks and Suchey, 1990), the pitted face, more than 'moderate' lipping of the dorsal border, marked porosity and developed osteophyte of the ventral surface (Fig. 6a,b,c, respectively) suggesting advanced degeneration (although only a limited portion of this ventral surface is preserved), are indicative of phase 6. This phase is associated with a mean age of 61.2 (± 12.2) years in the modern sample on which the standards were developed and a range of 34–86 years (Brooks and Suchey, 1990). Combining the Todd and Suchey-Brooks estimates, the evidence suggests an older adult aged around 40–50 years.

This age estimate fits well with published estimates of Shanidar 5's age at death, and is consistent with the new remains belonging to this individual. The age at death of Shanidar 5 was directly estimated using femoral histomorphology at 40 ± 6.7 years (Trinkaus and Thompson, 1987), refining a previous estimate of 35–50 years, based primarily on a comparative level of dental wear to Shanidar 3, whose age was in turn estimated using pubic symphysis and auricular surface morphology of the pelvis, extensive dental wear and degenerative joint disease (Trinkaus, 1983b).

*3.5. Estimated stature and body mass*

Stature (± standard error) estimated from the total length of the talus following Pablos et al. (2013a) is 167 (± 4) cm. This is consistent with stature estimates made from the long bones of Shanidar 5 by Trinkaus (1983b) using the regression equations of Trotter and Gleser (1952) for Euroamericans. These yielded estimates of 167.3 cm based on ulna length, 170.4 cm based on estimated femur length, and 168.8–171.3

cm based on estimated tibia length. Stature estimates from various talar measurements following Will and Stock (2015) were more variable, ranging from 156–170 cm. Apart from the estimate of 170 cm based on talar head length (M9), estimates were relatively low (156–165 cm; SOM Table S3). It should be noted that Will and Stock's equations were based on relatively small samples (n = 18–19), which may affect their reliability.

Body mass estimates from talar measurements following McHenry (1992) and Will and Stock (2015) were overall less consistent with published estimates for Shanidar 5 and Neanderthals more generally. Only one of the Will and Stock (2015) equations, again using length of the talar head (M9), gave a femoral head diameter comparable with the actual measurement of the Shanidar 5 femoral head (47.5 mm vs. 47.5 mm;:Trinkaus, 1983b) which produced a body mass estimate of 70.6 kg (Plavcan et al., 2014). Estimated body mass based on our estimated femoral head measurement is identical to that of Plavcan et al. (2014), since the same method was used to estimate body mass from femoral head diameter in both.

The McHenry (1992) ordinary least squares regression equation gave a body mass of 52.6 kg, while the equations from Will and Stock (2015) gave femoral head diameter estimates of 41.5–45.1 mm, in turn giving body mass estimates between 56.3 and 64.1 kg (SOM Table S4). Such body mass estimates are low compared with those for other Neanderthals (males: 73.65–84.9 kg, n = 7; females: 59.9–71.5 kg, n = 5; data on individuals with pelvic sex determination only, from Plavcan et al. 2014: Table 2), particularly as Shanidar 5 is thought to be male.

*3.6. Pathological changes to the skeleton*

Pathological lesions on the skeleton are limited to mild osteoarthritic changes to several joints (marginal lipping or osteophyte formation; Rogers and Waldron, 1995). The proximal joint surface of the pedal distal phalanx (SH16A 591) and the anterior margin of inferior surface of the thoracic vertebral body (SH16 269) demonstrate marginal osteophytes. The posterior calcaneal facet and the inferior edges of the medial and lateral facets of the right talus (SH15A 64.5 & 76.1), the talar articular surface of the right navicular (SH15A 69.2), and the posterior margin of the distal joint surface of the right tibia (SH15A 64.12) show marginal

lipping. Such changes could be secondary to trauma or simply due to high levels of biomechanical loading over a lifetime (Rogers and Waldron, 1995). Trinkaus (1983b) stated that Shanidar 5 shows relatively little evidence of pathological lesions, although noted mild osteoarthritic changes to the proximal right ulna, and the proximal articular facets of two right ribs. Similar to the new finds, there was no involvement of the subchondral bone in any of the joints showing osteophytes or lipping (Trinkaus, 1983b). These mild degenerative changes are generally common throughout the adult Shanidar Cave skeletons, though more pronounced in Shanidar 1, 3 and 4 than in Shanidar 5, and interpreted as reflecting an active lifestyle (except in cases of clear trauma, e.g., Shanidar 1; Trinkaus, 1983b).

**4. Discussion and conclusions**

Shanidar 5 is an adult male Neanderthal, previously estimated to have been aged over 40 years at death (Trinkaus, 1977, 1983b), and to date to approximately 46–50 ka (Solecki, 1971; Cowgill et al., 2007). The skeleton was only partially recovered during Solecki's excavations, and was missing the mandible and most of the teeth, both humeri, the left radius, parts of both hands, most of the vertebrae, portions of the pelvis, the lower right leg, and both feet (Trinkaus, 1983b). The newly discovered hominin remains from the area of the original Shanidar 5 discovery principally consist of elements from the lower limb (left hip region, right lower leg and foot) and a smaller number of fragments from the axial skeleton and wrist. The new remains are metrically and morphologically consistent with being from *H. neanderthalensis* rather than *H. sapiens*, and a lack of duplicated elements, partial articulation of some remains (pelvis-femur, tibia/fibula-tarsals), and generally large and robust morphology indicate a single individual is represented.

Furthermore, multiple lines of evidence strongly support the attribution of the remains to Shanidar 5. First, the physical location of the new remains was directly below and adjacent to the original Shanidar 5 discovery (Fig. 2). Second, the approximate articulation of the new finds, their degree of preservation, evidence of disturbance, and positioning among stones are also consistent with descriptions of the original finds. Third, the remains do not duplicate any of the skeletal elements previously described for Shanidar 5 (Fig. 13), but complement and complete previously-described remains (e.g., the left femur). Fourth, the

new remains and Shanidar 5 share a generally large and robust morphology with evidence of mild degenerative changes affecting some joints. Unfortunately, it is not possible to directly compare or attempt to match the new remains with those from the previous excavations, as the latter were held in the Iraq Museum, Baghdad, and it remains unconfirmed whether they are still there following recent conflict in the region and known sacking of and damage to its museums. It was rare that the antimere of the new remains was sufficiently well preserved for Shanidar 5 to allow direct metric and morphological comparisons with the published material, but the metric comparisons of the new left hamate with data on the right hamates from Shanidar Cave are consistent with the bone belonging to Shanidar 5, but not Shanidar 3. Fifth, the age at death estimated from the newly-described partial pubic symphysis, which must be treated cautiously given methodological limitations discussed above, is nonetheless consistent with estimates for Shanidar 5 obtained by other methods.

[FIGURE 13 NEAR HERE]

Finally, stature estimated from talus length using Pablos et al. (2013a) and stature and body mass estimated from talar head length (but not other talar measurements) using Will and Stock (2015), are highly consistent with those previously published for Shanidar 5. However, estimates based on other talar measurements using equations from McHenry (1992) and Will and Stock (2015) appear to significantly underestimate stature and body mass in this individual compared with estimates derived from more standard techniques (Trinkaus, 1983b; Plavcan et al., 2014). This may relate to small sample size in the reference samples, and/or the fact they are comprised of recent individuals of *H. sapiens* who differ in skeletal proportions from Neanderthals. Further work is required to evaluate methods for estimating body size from the talus in Neanderthals and other hominins.

The cumulative evidence suggests very strongly that the new remains from Shanidar Cave belong to Shanidar 5. The excavation of these remains using modern techniques and sampling for sediment micromorphology, palynology and other laboratory analyses will offer new insights into the burial process and taphonomic conditions under which the remains were deposited, enabling any new evidence to contribute to the debates regarding the circumstances (cultural or otherwise) by which this individual was deposited in the cave. Currently we can say little about cause of death. Distinguishing between peri- and

post-mortem breaks is possible (e.g., Villa and Mahieu, 1991; L'Abbé et al., 2015; Sala et al., 2015) but would require a detailed analysis of all the old and new remains focusing on this question. Confirming death due to rock fall would still be challenging given that the remains are incomplete, often fragile and variably preserved. If rocks fell on the skeleton sometime after death, this could have led to the crushing of the remains that is observed, and the remains have clearly slumped and shifted from anatomical articulation, so it is also difficult to infer what was their original position. However, we hope that micromorphological analysis of sediment blocks taken during the excavation of the new finds will help elucidate the circumstances of the placement of the Shanidar 5 remains in the context of the argument that the individual was killed by rockfall. The recent finds also offer new evidence regarding the age at death of Shanidar 5 and the potential for novel analyses, such as ancient DNA or bone microstructure, that were not possible on the original remains, which are now inaccessible. Finally, the new elements add to the available datasets on Neanderthal morphology, and contribute to strengthening future analyses and interpretations of these data.

**Acknowledgements**

This work was supported by the Leverhulme Trust (RPG-2013-105, held by GB). EP is supported by the Leverhulme (ECF-2015-520) and Isaac Newton Trusts. MML's and FC's research is supported by the European Research Council (ERC #295907). The new fieldwork at Shanidar Cave is directed by GB and is being undertaken with the permission of the Kurdistan General Directorate of Antiquities, which is warmly thanked—in particular, the General Director Mala Awat and the Directorate's Representative on the project, Dlshad Abdulmutalb, for his continued support and input into the fieldwork. Thanks to Ross Lane for assistance with the plans in Figure 1. EP thanks Professor Erik Trinkaus for his advice and assistance, as well as Jay Stock and Asier Gómez for helpful discussion, and Adrián Pablos for discussions and for kindly sharing unpublished data. The financial support of the Leverhulme Trust (Research Grant RPG-2013-105 held by GB) is also gratefully acknowledged. We also thank the Editor, Associate Editor and two anonymous reviewers for constructive feedback that helped to improve the article.

**References**


Anton, S.C., 1997. Endocranial hyperostosis in Sangiran 2, Gibraltar 1, and Shanidar 5. Am. J. Phys. Anthropol. 102, 111–122.

Auerbach, B.M., Ruff, C.B., 2010. Stature estimation formulae for indigenous North American populations. Am. J. Phys. Anthropol. 141, 190–207.

Baba, H., Endo, B., 1982. Postcranial skeleton of the Minatogawa man. In: Suzuki, H., Hanihara, K. (Eds.), The Minatogawa Man: The Upper Pleistocene Man from the Island of Okinawa. University of Tokyo Press, Tokyo, pp.61–195 .

Bastir, M., García Martínez, D., Rios, L., Higuero, A., Barash, A., Martelli, S., García Tabernero, A., Estalrrich, A., Huguet, R., de la Rasilla, M., Rosas, A., 2017. Three-dimensional morphometrics of thoracic vertebrae in Neandertals and the fossil evidence from El Sidrón (Asturias, Northern Spain). J. Hum. Evol. 108, 47–61.

Berger, T.D., Trinkaus, E., 1995. Patterns of trauma among the Neandertals. J. Arch. Sci. 22, 841–852.

Billy, G., 1969. Le squelette post-crânien de l'Homme de Chancelade. L'Anthropologie 73, 207–246.

Billy, G., 1975. Étude anthropologique des restes humains de l'Abri Pataud. In: Movius, H.L. (Ed.), Excavation of the Abri Pataud Les Eyzies (Dordogne). Peabody Museum of Archaeology and Ethnology, Harvard University, Cambridge, MA, pp. 201–261.

Bräuer, G., 1988. Osteometrie. In: Knussman, R. (Ed.), Anthropologie: Handbuch der Vergleichenden Biologie des Menchen. Gustav Fisher, Stuttgart, pp. 160–232.

Brooks, S., Suchey, J., 1990. Skeletal age determination based on the os pubis: A comparison of the Acsádi-Nemeskéri and Suchey-Brooks methods. Hum. Evol. 5, 227–238.

Buikstra, J.E., Ubelaker, D.H., 1994. Standards for Data Collection from Human Skeletal Remains. Arkansas Archaeological Survey Research Series No. 44, Fayetteville.

Capasso, L., Kennedy, K.A.R., Wilczak, C.A., 1999. Atlas of Occupational Markers on Human Remains. Edigrafital, Teramo.

Carretero, J.M., Quam, R.M., Gómez-Olivencia, A., Castilla, M., Rodríguez, L., García-González, R., 2015. The Magdalenian human remains from El Mirón Cave, Cantabria (Spain). J. Arch. Sci. 60, 10–27.

Chech, M., Grove, C.P., Thorne, A., Trinkaus, E., 1999. A new reconstruction of the Shanidar 5 cranium. Paléorient 25, 143–146.

Churchill, S.E., Franciscus, R.G., McKean-Peraza, H.A., Daniel, J.A., Warren, B.R., 2009. Shanidar 3 Neandertal rib puncture wound and Paleolithic weaponry. J. Hum. Evol. 57, 163–178.

Clark, J.L., Dobson, S.D., Antón, S., Hawks, J., Hunley, K., Wolpoff, M., 2007. Identifying artificially deformed crania. Int. J. Osteoarch. 17, 596–607.

Corrain, C., 1977. I resti scheletrici della sepoltura epi-Gravettiana del `Riparo Tagliente' in Valpantena (Verona). Boll. Mus. Civ. Stor. Nat. Verona 4, 35–79.

Cowgill, L.W., Trinkaus, E., Zeder, M.A., 2007. Shanidar 10: A Middle Paleolithic immature distal lower limb from Shanidar Cave, Iraqi Kurdistan. J. Hum. Evol. 53, 213–223.

Crevecoeur, I., 2008. Étude Anthropologique du Squelette du Paléolithique Supérieur de Nazlet Khater 2 (Égypte): Apport à la Compréhension de la Variabilité Passée des Hommes Modernes. Leuven University Press, Leuven.

Crubézy, E., Trinkaus, E., 1992. Shanidar 1: A case of hyperostotic disease (DISH) in the middle paleolithic. Am. J. Phys. Anthropol. 89, 411–420.

Dettwyler, K.A., 1991. Can paleopathology provide evidence for “compassion”? Am. J. Phys. Anthropol. 84, 375–384.

Digiovanni, B.F., Scoles, P.V., Latimer, B.M., 1989. Anterior extension of the thoracic vertebral bodies in Scheuermann's kyphosis: An anatomic study. Spine 14, 712–716.

Endo, B., Kimura, T., 1970. Postcranial skeleton of the Amud man. In: Suzuki, H., Takai, F. (Eds.), The Amud Man and His Cave Site. Academic Press of Japan, Tokyo, pp. 231–426.

Feldesman, M.R., Lundy, J.K., 1988. Stature estimates for some African Plio-Pleistocene fossil hominids. J. Hum. Evol. 17, 583–596.

Fraipont, C., 1913. Sur l´importance des caracteres de l´astragale chez l´homme fossile. Bull. Soc. Anthropol. Bruxelles 32, 145–208.

Gargett, R.H., 1999. Middle Palaeolithic burial is not a dead issue: the view from Qafzeh, Saint-Césaire, Kebara, Amud, and Dederiyeh. J. Hum. Evol. 37, 27–90.

Gómez-Olivencia, A., Been, E., Arsuaga, J.L., Stock, J.T., 2013a. The Neandertal vertebral column 1: The cervical spine. J. Hum. Evol. 64, 608–630.

Gómez-Olivencia, A., Couture-Veschambre, C., Madelaine, S., Maureille, B., 2013b. The vertebral column of the Regourdou 1 Neandertal. J. Hum. Evol. 64, 582–607.

Grine, F.E., Jungers, W.L., Tobias, P.V., Pearson, O.M., 1995. Fossil *Homo* femur from Berg Aukas, northern Namibia. Am. J. Phys. Anthropol. 97, 151–185.

Harvati, K., Darlas, A., Bailey, S.E., Rein, T.R., El Zaatari, S., Fiorenza, L., Kullmer, O., Psathi, E., 2013. New Neanderthal remains from Mani peninsula, Southern Greece: The Kalamakia Middle Paleolithic cave site. J. Hum. Evol. 64, 486–499.

Heim, J.L., 1982. Les Hommes Fossiles de la Ferrassie. Tome II. Les Squelettes Adultes (Squelettes des Membres). Masson, Paris.

Henry, A.G., Brooks, A.S., Piperno, D.R., 2011. Microfossils in calculus demonstrate consumption of plants and cooked foods in Neanderthal diets (Shanidar III, Iraq; Spy I and II, Belgium). Proc. Natl. Acad. Sci. 108, 486–491.

Holliday, T.W., Ruff, C.B., 1997. Ecogeographical patterning and stature prediction in fossil hominids: Comment on M.R. Feldesman and R.L. Fountain, American Journal of Physical Anthropology (1996) 100:207-224. Am. J. Phys. Anthropol. 103, 137–140.

Kivell, T.L., Barros, A.P., Smaers, J.B., 2013. Different evolutionary pathways underlie the morphology of wrist bones in hominoids. BMC Evol. Biol. 13, 229.

L'Abbé, E.N., Symes, S.A., Pokines, J.T., Cabo, L.L., Stull, K.E., Kuo, S., Raymond, D.E., Randolph-Quinney, P.S., Berger, L.R., 2015. Evidence of fatal skeletal injuries on Malapa Hominins 1 and 2. Sci. Rep. 5, 15120.

Leroi-Gourhan, A., 1975. The flowers found with Shanidar IV, a Neanderthal burial in Iraq. Science 190, 562–564.

Lorenzo, C., Arsuaga, J.L., Carretero, J.M., 1999. Hand and foot remains from the Gran Dolina Early Pleistocene site (Sierra de Atapuerca, Spain). J. Hum. Evol. 37, 501–522.

Lu, Z., Meldrum, D.J., Huang, Y., He, J., Sarmiento, E.E., 2011. The Jinniushan hominin pedal skeleton from the late Middle Pleistocene of China. Homo 62, 389–401.

Martín-González, J.A., Mateos, A., Goikoetxea, I., Leonard, W.R., Rodríguez, J., 2012. Differences between Neandertal and modern human infant and child growth models. J. Hum. Evol. 63, 140–149.

Martin, R., Saller, K., 1957. Lehrbuch der Anthropologie. Fischer, Stuttgart.

Matiegka, J., 1938. Homo Předmostensis, Fosilní Člověk z Předmostí na Moravě II: Ostaní Části Kostrové. České Akademie Věd a Umění, Prague.

Mays, S., 2015. The effect of factors other than age upon skeletal age indicators in the adult. Ann. Hum. Biol. 42, 332–341.

McCown, T.D., Keith, A., 1939. The Stone Age of Mount Carmel Volume 2: The Fossil Human Remains from the Levalloiso-Mousterian. AMS Press, New York.

McDermott, F., Grun, R., Stringer, C.B., Hawkesworth, C.J., 1993. Mass-spectrometric U-series dates for Israeli Neanderthal/early modern hominid sites. Nature 363, 252–255.

McHenry, H.M., 1992. Body size and proportions in early hominids. Am. J. Phys. Anthropol. 87, 407–431.

Mersey, B., Jabbour, R.S., Brudvik, K., Defleur, A., 2013. Neanderthal hand and foot remains from Moula-Guercy, Ardèche, France. Am. J. Phys. Anthropol. 152, 516–529.

Molleson, T., Cox, M., 1993, The Spitalfields Project, Volume 2: The Anthropology: The Middling Sort. CBA Research Report 86. Council for British Archaeology, York.

Niewoehner, W.A., Weaver, A.H., Trinkaus, E., 1997. Neandertal capitate-metacarpal articular morphology. Am. J. Phys. Anthropol. 103, 219–233.

Pablos, A., Lorenzo, C., Martínez, I., Bermúdez de Castro, J.M., Martinón-Torres, M., Carbonell, E., Arsuaga, J.L., 2012. New foot remains from the Gran Dolina-TD6 Early Pleistocene site (Sierra de Atapuerca, Burgos, Spain). J. Hum. Evol. 63, 610–623.

Pablos, A., Gómez-Olivencia, A., García-Pérez, A., Martínez, I., Lorenzo, C., Arsuaga, J.L., 2013a. From toe to head: Use of robust regression methods in stature estimation based on foot remains. Forensic Sci. Int. 226, 299.e1–229.e7.

Pablos, A., Martínez, I., Lorenzo, C., Gracia, A., Sala, N., Arsuaga, J.L., 2013b. Human talus bones from the Middle Pleistocene site of Sima de los Huesos (Sierra de Atapuerca, Burgos, Spain). J. Hum. Evol. 65, 79–92.

Pablos, A., Pantoja-Pérez, A., Martínez, I., Lorenzo, C., Arsuaga, J.L., 2017a. Metric and morphological analysis of the foot in the Middle Pleistocene sample of Sima de los Huesos (Sierra de Atapuerca, Burgos, Spain). Quat. Int. 433, 103–113.

Pablos, A., Sala, N., Arribas, A., 2017b. Taxonomic reassignment of the Paleolithic human navicular from Cueva de los Torrejones (Guadalajara, Spain). Archaeol. Anthropol. Sci. DOI: 10.1007/s12520-017-0503-8

Paoli, G., Parenti, R., Sergi, S., 1980. Gli scheletri mesolitici della Caverna delle Arene Candide (Liguria). Mem. Ist. Ital. Paleontol. Um. 3, 33–154.

Pardini, E., Lombardi Pardini, E.C., 1981. I Paleolitici di Vado all'Arancio (Grosseto). Archiv. Antropol. Etnol. Firenze 111, 75–119.

Patte, E., 1968. L'Homme et la Femme de l'Azilien de Saint-Rabier. Mém. Mus. Natl. Hist. Nat. C 19, 1–56.

Pearson, K., 1899. Mathematical Contributions to the Theory of Evolution. V. On the Reconstruction of the Stature of Prehistoric Races. Phil. Trans. Royal Soc. Lond. A. 192, 169–244.

Pearson, O.M., 2000. Activity, climate, and postcranial robusticity - Implications for modern human origins and scenarios of adaptive change. Curr. Anthropol. 41, 569–607.

Pearson, O.M., Cordero, R.M., Busby, A.M., 2006. How different were Neanderthals' habitual activities? A comparative analysis with diverse groups of recent humans. In: Hublin, J.-J., Harvati, K., Harrison, T. (Eds.), Neanderthals Revisited: New Approaches and Perspectives. Springer Netherlands, Dordrecht, pp. 135–156.

Pearson, O.M., Royer, D.F., Grine, F.E., Fleagle, J.G., 2008. A description of the Omo I postcranial skeleton, including newly discovered fossils. J. Hum. Evol. 55, 421–437.

Plavcan, J. M., Meyer, V., Hammond, A. S., Couture, C., Madelaine, S., Holliday, T. W., Maureille, B., Ward, C.V., Trinkaus, E., 2014. The Regourdou 1 Neandertal body size. C. R. Palevol. 13, 747–754.

Porter, A. M. W., 2002. Estimation of body size and physique from hominin skeletal remains. Homo 53, 17–38.

Pomeroy, E., Stock, J.T., 2012. Estimation of stature and body mass from the skeleton among coastal and mid-altitude Andean populations. Am. J. Phys. Anthropol. 147, 264–279.

Rak, Y., 1990. On the differences between two pelvises of Mousterian context from the Qafzeh and Kebara caves, Israel. Am. J. Phys. Anthropol. 81, 323–332.

Rak, Y., Arensburg, B., 1987. Kebara 2 Neanderthal pelvis: First look at a complete inlet. Am. J. Phys. Anthropol. 73, 227–231.

Reynolds, T., Boismier, W., Farr, L., Hunt, C., Abdulmultalb, D., Barker, G., 2015. New investigations at Shanidar Cave, Iraqi Kurdistan. Antiquity 348, Project Gallery, http://antiquity.ac.uk/projgall/barker348 [Accessed 31/01/2017].

Reynolds, T., Boismier, W., Farr, L., Hunt, C., Abdulmutalb, D., Barker, G, 2016. New investigations at Shanidar Cave, Iraqi Kurdistan. In: Kopanias, K., MacGinnis, J. (Eds.), The Archaeology of the Kurdistan Region of Iraq and Adjacent Regions. Archaeopress, Oxford, pp. 357–360.

Rhoads, J.G., Trinkaus, E., 1977. Morphometrics of the Neandertal talus. Am. J. Phys. Anthropol. 46, 29–43.

Rogers, J., Waldron, T., 1995. A Field Guide to Joint Disease in Archaeology. John Wiley and Sons, Chichester.

Ruff, C.B., 2010. Body size and body shape in early hominins - implications of the Gona Pelvis. J. Hum. Evol. 58, 166–178.

Ruff, C.B., Scott, W.W., Liu, A.Y., 1991. Articular and diaphyseal remodeling of the proximal femur with changes in body mass in adults. Am. J. Phys. Anthropol. 86, 397–413.

Ruff, C.B., Trinkaus, E., Walker, A., Larsen, C.S., 1993. Postcranial robusticity in *Homo*. I: Temporal trends and mechanical interpretation. Am. J. Phys. Anthropol. 91, 21–53.

Ruff, C.B., Holt, B.M., Niskanen, M., Sladék, V., Berner, M., Garofalo, E., Garvin, H.M., Hora, M., Maijanen, H., Niinimäki, S., Salo, K., Schuplerová, E., Tompkins, D., 2012. Stature and body mass estimation from skeletal remains in the European Holocene. Am. J. Phys. Anthropol. 148, 601–617.

Sala, N., Arsuaga, J.L., Martínez, I., Gracia-Téllez, A., 2015. Breakage patterns in Sima de los Huesos (Atapuerca, Spain) hominin sample. J. Arch. Sci. 55, 113–121.

Schmitt, A., Murail, P., Cunha, E., Rougé, D., 2002. Variability of the pattern of aging on the human skeleton: evidence from bone indicators and implications on age at death estimation. J. Forensic Sci. 47, 1203–1209.

Shang, H., Trinkaus, E., 2010. The Early Modern Human from Tianyuan Cave, China. Texas A&M University Press, College Station, TX.

Sládek, V., Trinkaus, E., Hillson, S.W., Holliday, T.W., 2000. The People of the Pavlovian: Skeletal Catalogue and Osteometrics of the Gravettian Fossil Hominids from Dolní Věstonice and Pavlov. Academy of Sciences of the Czech Republic, Institute of Archaeology.

Solecki, R.S., 1961. New anthropological discoveries at Shanidar, Northern Iraq. Trans. New York Acad. Sci. 23, 690–699.

Solecki, R.S., 1963. Prehistory in Shanidar Valley, Northern Iraq. Science 139, 179–193.

Solecki, R.S., 1971. Shanidar: The First Flower People. Alfred A. Knopf Inc., New York.

Solecki, R.S., 1975. Shanidar IV, a Neanderthal flower burial in Northern Iraq. Science 190, 880–881.

Sommer, J.D., 1999. The Shanidar IV 'flower burial': a re-evaluation of Neanderthal burial ritual. Camb. Archaeol. J. 9, 127–129.

Stewart, T.D., 1960. Form of the pubic bone in Neanderthal man. Science 131, 1437–1438.

Stewart, T.D., 1969. Fossil evidence of human violence. Trans-action 6, 48–53.

Stewart, T.D., 1977. The Neanderthal skeletal remains from Shanidar Cave, Iraq: A summary of findings to date. Proc. Am. Philos. Soc. 121, 121–165.

Todd, T.W., 1920. Age changes in the pubic bone. I. The male white pubis. Am. J. Phys. Anthropol. 3, 285–334.

Todd, T.W., 1921. Age changes in the pubic bone. Am. J. Phys. Anthropol. 4, 1–70.

Trinkaus, E., 1975a. A functional analysis of the Neanderthal foot. Ph.D. Dissertation, University of Pennsylvania.

Trinkaus, E., 1975b. Squatting among the Neandertals: A problem in the behavioral interpretation of skeletal morphology. J. Arch. Sci. 2, 327–351.

Trinkaus, E., 1976. The morphology of European and Southwest Asian Neandertal pubic bones. Am. J. Phys. Anthropol. 44, 95–103.

Trinkaus, E., 1977. The Shanidar 5 Neanderthal skeleton. Sumer 33, 35–41.

Trinkaus, E., 1981. Neanderthal limb proportions and cold adaptation. In: Stringer, C.B. (Ed.), Aspects of Human Evolution. Taylor and Francis, London, pp. 187–224.

Trinkaus, E., 1982. Artificial Cranial Deformation in the Shanidar 1 and 5 Neandertals. Curr. Anthropol. 23, 198–199.

Trinkaus, E., 1983a. Functional aspects of Neandertal pedal remains. Foot Ankle Int. 3, 377–390.

Trinkaus, E., 1983b. The Shanidar Neandertals. Academic Press, New York.

Trinkaus, E., 2000. The human remains from Paviland Cave. Late Pleistocene and Holocene human remains from Paviland Cave. In: Aldhouse-Green, S. (Ed.), Paviland Cave and the 'Red Lady'. A Definitive Report. Western Academic & Specialist Press, Bristol, pp. 141–199.

Trinkaus, E., Buzhilova, A.P., Mednikova, M.B., Dobrovolskaya, M.V., 2014. The People of Sunghir: Burials, Bodies, and Behavior in the Earlier Upper Paleolithic. Oxford University Press, Oxford.

Trinkaus, E., Rhoads, M.L., 1999. Neandertal knees: power lifters in the Pleistocene? J. Hum. Evol. 37, 833–859.

Trinkaus, E., Thompson, D.D., 1987. Femoral diaphyseal histomorphometric age determinations for the Shanidar 3, 4, 5, and 6 Neandertals and Neandertal longevity. Am. J. Phys. Anthropol. 72, 123–129.

Trinkaus, E., Zimmerman, M.R., 1982. Trauma among the Shanidar Neandertals. Am. J. Phys. Anthropol. 57, 61–76.

Trotter, M., 1970. Estimation of stature from intact long bones. In: Stewart, T.D. (Ed.), Personal Identification in Mass Disasters. Smithsonian Institution, Washington, pp. 71–83.

Trotter, M., Gleser, G.C., 1952. Estimation of stature from long bones of American whites and negroes. Am. J. Phys. Anthropol. 10, 463–514.

Vandermeersch, B., 1981. Les Hommes Fossiles de Qafzeh (Israël). Editions du Centre National de la Recherche Scientifique, Paris.

Villa, P., Mahieu, E., 1991. Breakage patterns of human long bones. J. Hum. Evol. 21, 27–48.

Walker, M.J., Ortega, J., López, M.V., Parmová, K., Trinkaus, E., 2011. Neandertal postcranial remains from the Sima de las Palomas del Cabezo Gordo, Murcia, southeastern Spain. Am. J. Phys. Anthropol. 144, 505–515.

Weaver, T.D., 2009. The meaning of Neandertal skeletal morphology. Proc. Natl. Acad. Sci. 106, 16028–16033.

White, T.D., Black, M.T., Folkens, P.A., 2011. Human Osteology, 3rd Edition. Academic Press, London.

Will, M., Stock, J.T., 2015. Spatial and temporal variation of body size among early *Homo*. J. Hum. Evol. 82, 15–33.

**Figures**

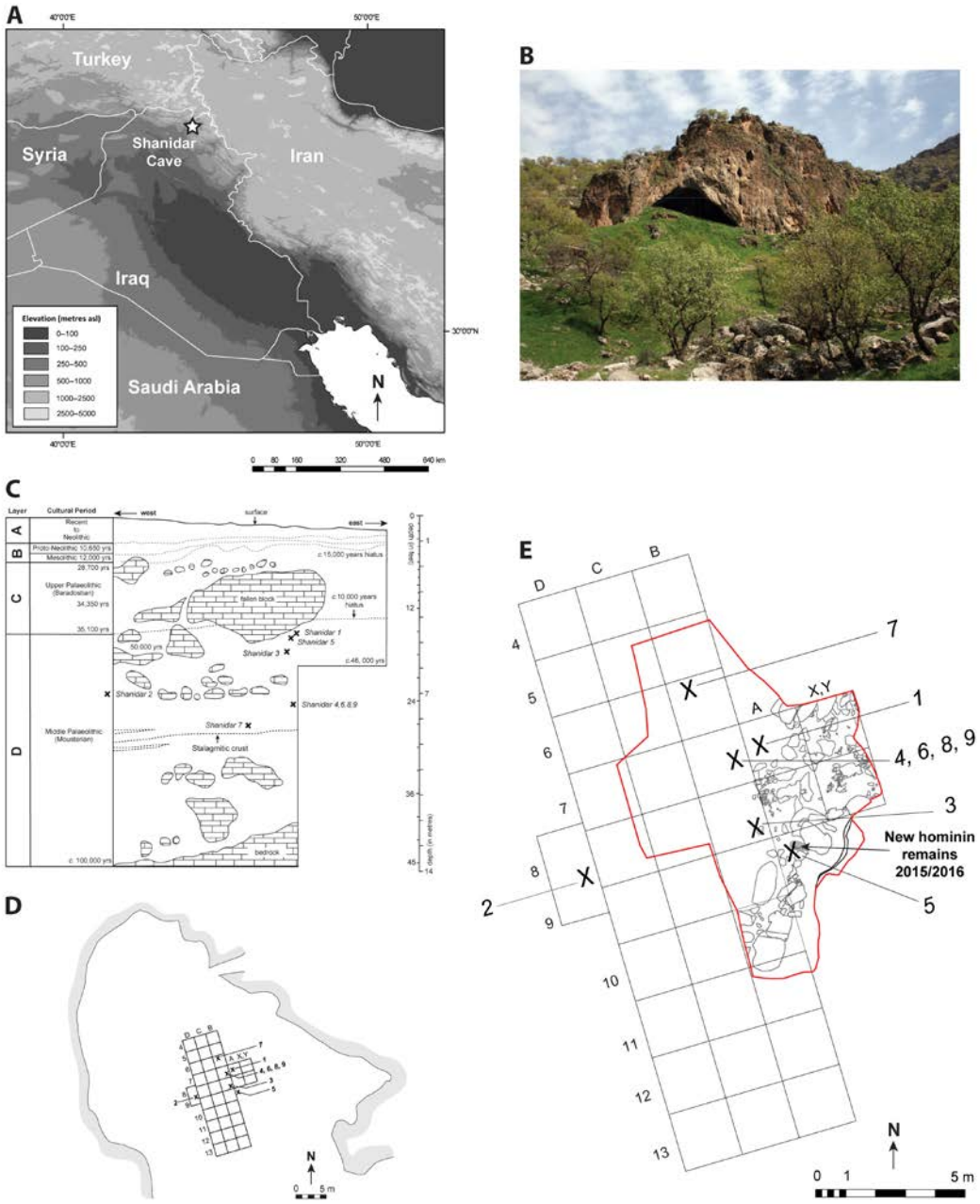


**Figure 1.** The Shanidar Cave excavations. A: Map showing the location of Shanidar Cave. B: Entrance to Shanidar Cave, viewed from the south. C: Schematic stratigraphy from Ralph Solecki's excavations (redrawn from Stewart, 1977: Figure 2, with modifications). D: Plan of Shanidar Cave showing the location of Solecki's excavation grid (based on Stewart, 1977: Figure 1, and survey data from the current project). E: Enlarged plan of Solecki's excavation grid, showing the location of the Neanderthal remains (numbered), the 2015–2016 excavations (red outline, with major rocks outlined in gray), and the hominin remains found in 2015–2016 (shaded gray), which we describe and attribute to Shanidar 5 in this paper.

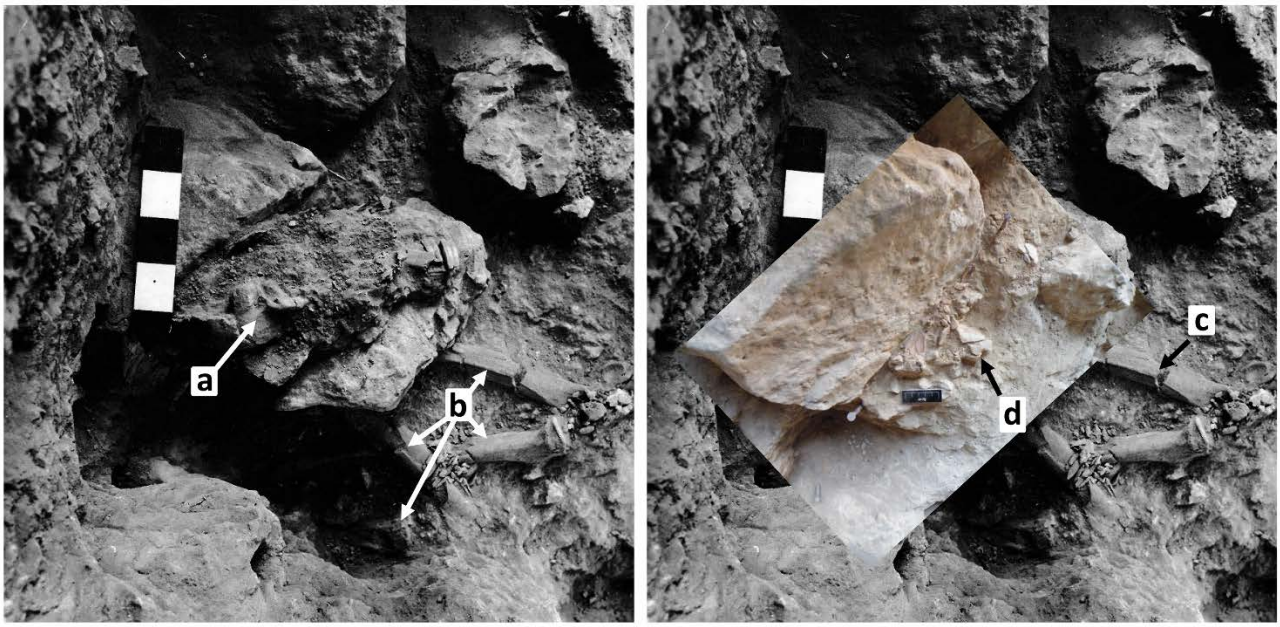


**Figure 2.** Photograph of the Shanidar 5 lower limbs in situ (left), overlaid with a photo of the 2016 left hip remains in situ (right). The images illustrate the matching topography of the rocks in both pictures and indicate that the 2016 left hip lay directly adjacent to the original Shanidar 5 lower limb finds. The skull (a) was on top of a rock, and the pelvis (not shown) and lower limb remains (b) underneath. The more distal section of the left femoral shaft found in 1960 (c) aligns closely with the proximal section of the shaft found in 2016 (d). Length of black scale bar in inset photo = 5 cm. (Black and white photograph: Trinkaus, 1977: Figure 1, courtesy of R. Solecki).

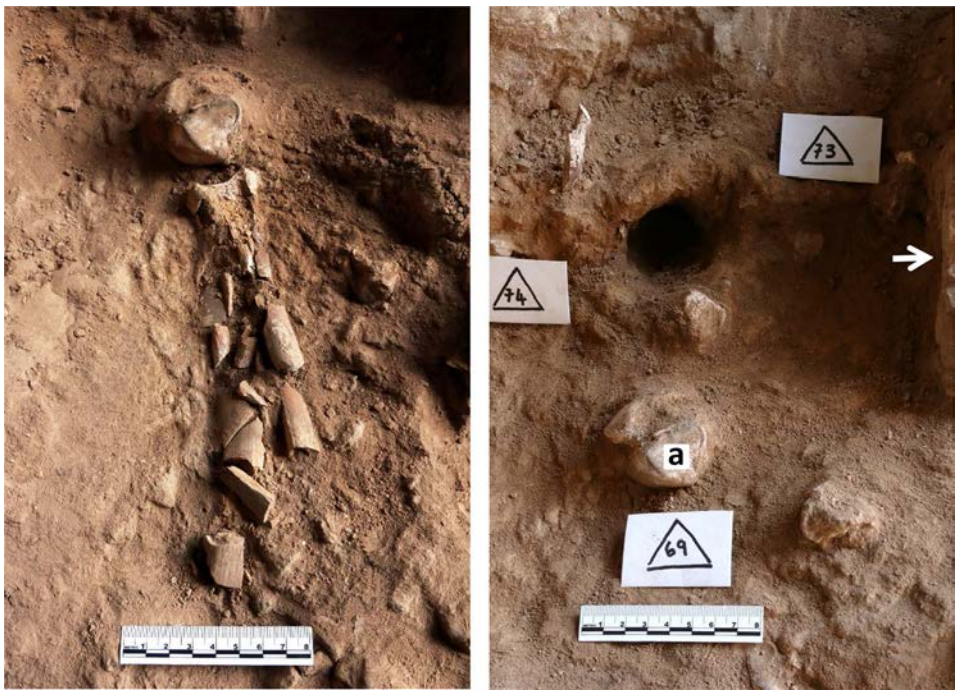


**Figure 3.** Remains of the right tibia, fibula, and talus as discovered at Shanidar Cave in 2015. Left: the talus, tibia and fibula remains. North is towards the upper left corner of the picture, where there is also a rodent burrow that likely disturbed the rest of the right foot. Right: close-up showing the location of the burrow mentioned previously in relation to the talus (a). Arrow indicates the side of the rock, in front of which (i.e., in the region just out of frame in the lower right hand side of the photograph) the remains of the left proximal femur and pelvis were found in 2016. Scale in cm.

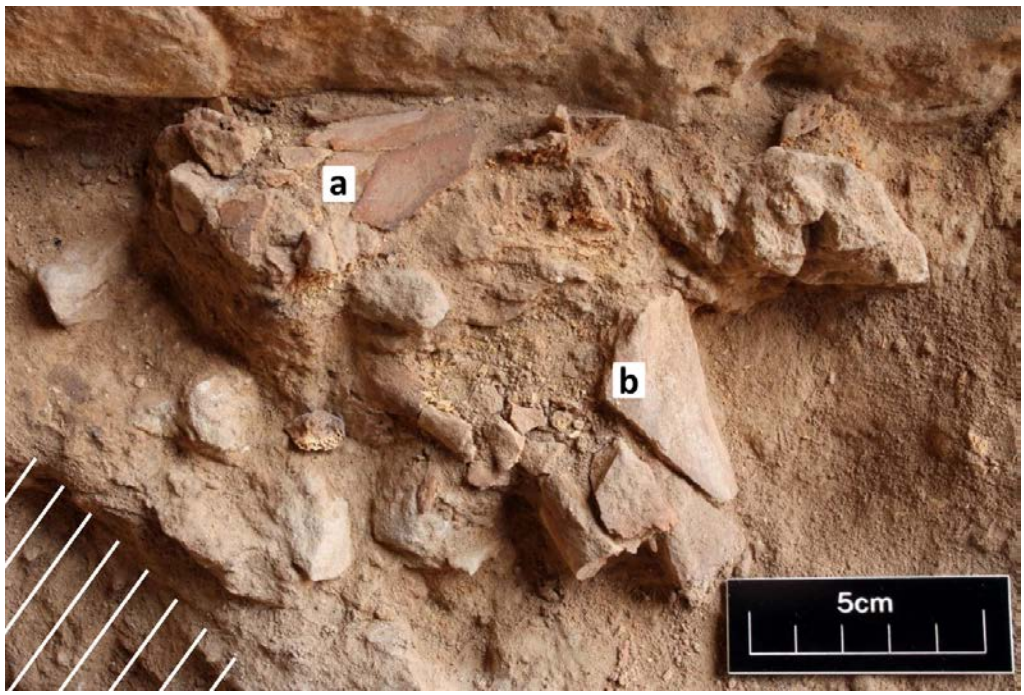


**Figure 4.** Remains of the pelvis (a) and proximal femur (b) discovered at Shanidar Cave in 2016. North is to the left, and the base of the rock lying tight against the remains can be seen in the top of the image. The hatched area (bottom left) was removed as part of the block containing the right tibia and fibula during the previous excavation season.

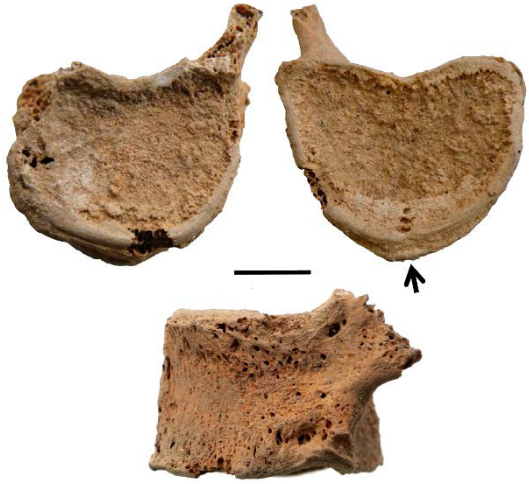

**Figure 5.** Adult thoracic vertebral body (SH16 269) from Shanidar Cave. Upper left: superior; upper right: inferior; below: left lateral. Arrow indicates anterior extension of the inferior surface. Scale bar = 10 mm.


**Figure 6.** Reconstructed left pubic symphysis (SH16 239.1) from Shanidar Cave**.** Only three fragments forming part of the pubic symphysis itself are illustrated. (a) continuous osteophytic outgrowth along dorsal border. (b) Porosity and degeneration of ventral surface. (c) Osteophyte on ventral surface. Ventral is to the right, dorsal to the left and superior at the top of the image. Scale bar = 10 mm.

**Figure 7.** Adult left hamate (SH15 590) from Shanidar Cave. Clockwise from top left: capitate articular surface; triquetral articular surface; palmar view; distal view; and dorsal view. Scale bar = 10 mm.

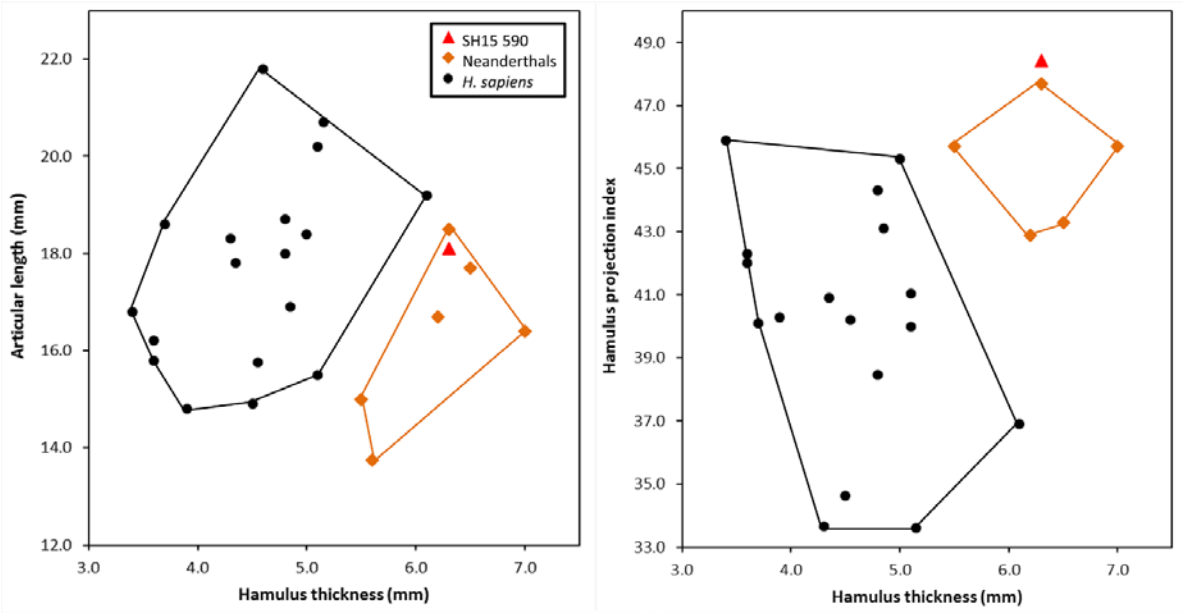


**Figure 8.** Bivariate plots of measurements from the SH15 590 left hamate from Shanidar Cave and comparative data from Neanderthals and *H. sapiens*. Left: Articular length against hamulus thickness. Right: Hamulus projection index against hamulus thickness. See Table 3 for detail of the comparative data**.**

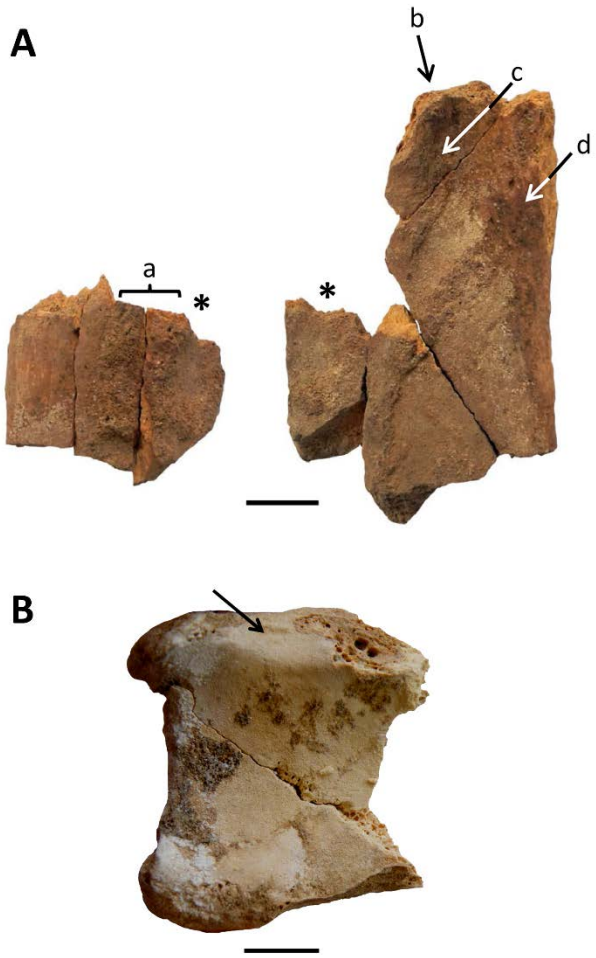


**Figure 9.** Adult left proximal femur (SH16 238) distal right tibial articular surface (SH15A 64.12) from Shanidar Cave. A: Proximal femur; upper left: three femoral fragments preserving part of gluteal tuberosity (a); upper right: four refitting fragments of the proximal femur showing the base of the lesser trochanter (c), pectineal line (b), and spiral line (d). Note that the fragment marked above with an asterisk features in both images. B: Inferior view of the right distal tibia; lateral is to the left, anterior towards the top; note the ankle flexion facet indicated by the arrow. Scale bar = 10 mm.

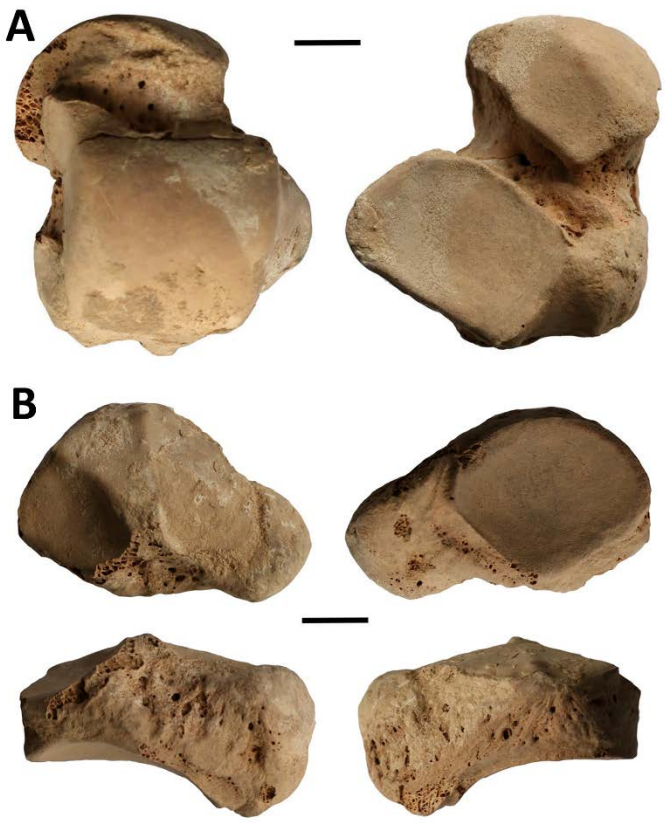


**Figure 10.** The right talus (SH15A 69.1) and right navicular (SH15A 69.2) from Shanidar Cave. A: talus in superior view (left) and inferior view (right). B: Navicular, clockwise from top left: distal, proximal, dorsal and plantar views. Scale bar = 10 mm.

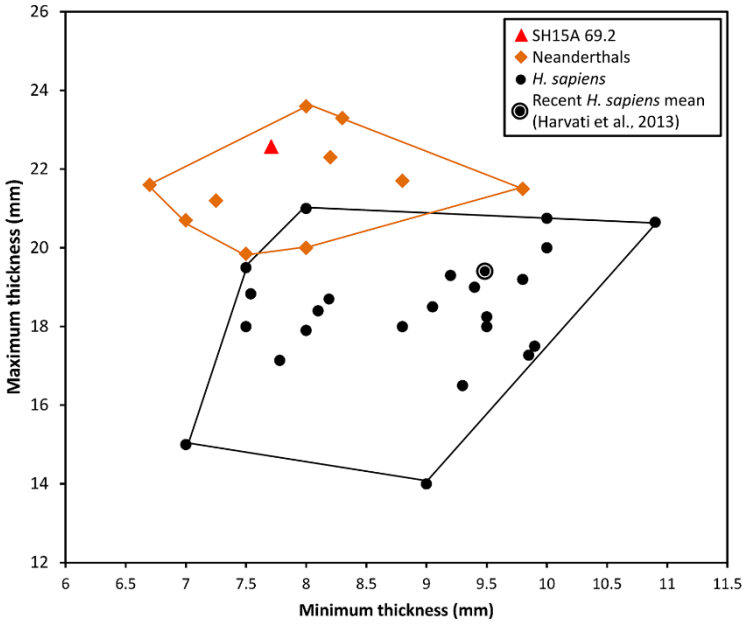


**Figure 11.** Plot of navicular maximum thickness against minimum thickness comparing SH15A 69.2 with other Neanderthals and *H. sapiens*. See Table 5 for details of the comparative data.

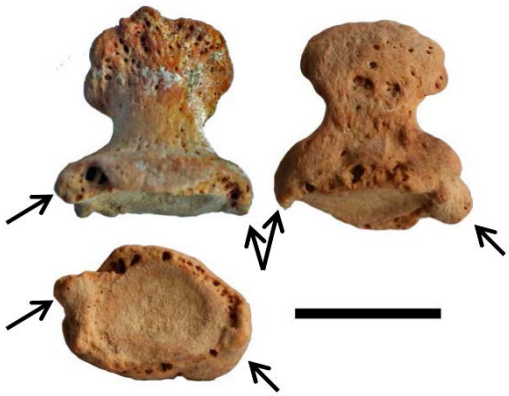

**Figure 12.** Distal pedal phalanx (SH16A 591) from Shanidar Cave. Clockwise from top left: dorsal, plantar, and proximal views. Arrows indicate marginal osteophytes around the joint surface. Scale bar = 10 mm.

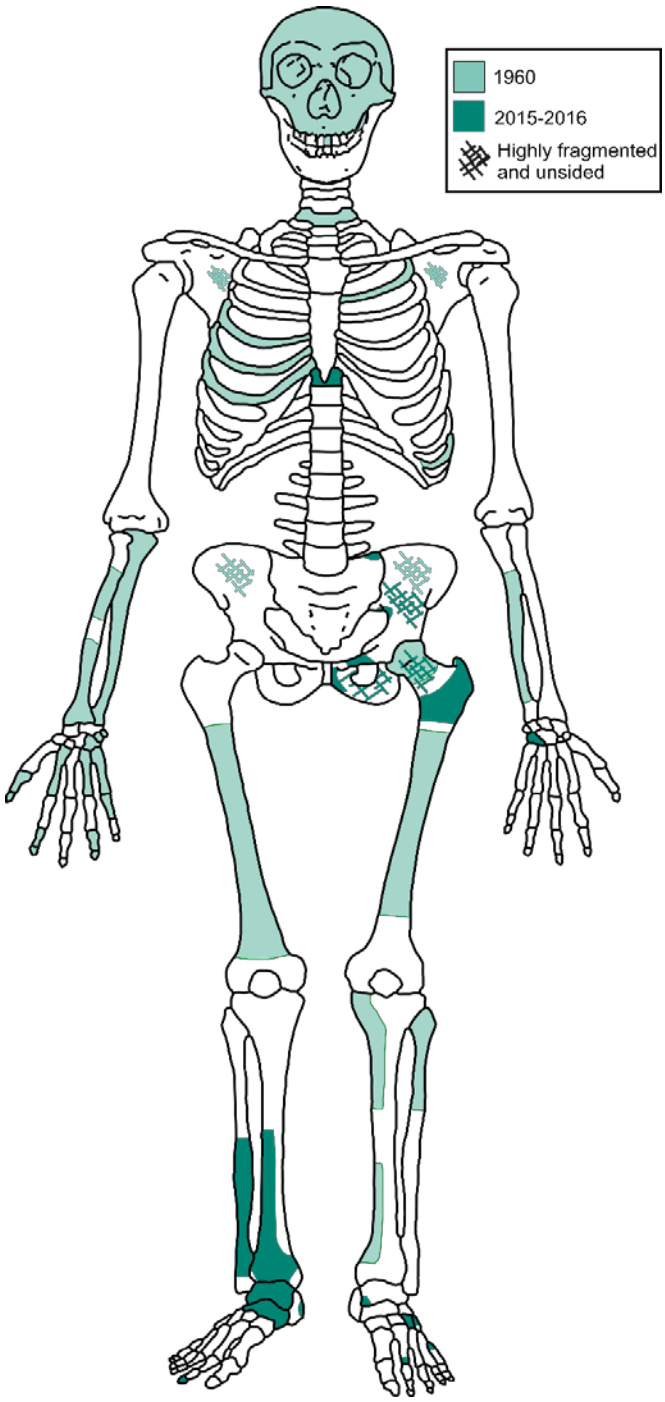


**Figure 13.** Schematic representation of the skeletal remains attributed to Shanidar 5 from the excavations in 1960 and 2015–2016. The areas marked as present (solid color) are not necessarily complete; for example, only the posterior part of the left femoral head and neck were recovered in 1960 by Ralph Solecki. Hatched areas denote fragmentary remains that could not be attributed to a specific side of the body. Note that there is no duplication of elements between the previously-described Shanidar 5 material and that recovered from our recent excavations.

## Tables

### Table 1

Inventory of skeletal remains from Shanidar Cave recovered in 2015 and 2016 from the vicinity of the original Shanidar 5 discovery.

| Specimen ID | Identification | Detail | Figure |
|---|---|---|---|
| **Axial skeleton and pelvic girdle** | | | |
| SH15A 72.2 | Vertebra, cervical | Left superior facet, probably upper subaxial cervical vertebra | S2 |
| SH15A 72.1 | Vertebra, thoracic | Mid-thoracic spinous process | S2 |
| SH15A 64.1 | Vertebra, thoracic? | Fragment of margin of vertebral body | S2 |
| SH16 269 | Vertebra, thoracic | Vertebral body, complete | 5 |
| SH15A 64.4 | Sacrum | Fragment of posterior part of left ala | S2 |
| SH16 239.1 | Os coxae (left) | Partial pubic symphysis | 6 |
| SH16 239.2 | Os coxae (left) | Superior pubic ramus | S2 |
| SH16 239.3 | Os coxae (unsided) | Part of margin of obturator foramen | S2 |
| SH16 245.3 | Os coxae (left) | Anterior part of pubic ramus near to the acetabulum | S2 |
| SH16 245.4 | Os coxae (unsided) | Fragment of margin of obturator foramen | S2 |
| SH16 278 | Os coxae (unsided) | Fragments of ilium | S2 |
| SH15A 65 | Os coxae (left) | Fragment of greater sciatic notch | S2 |
| **Upper Limb** | | | |
| SH15 590 | Left hamate | Largely complete | 7, S3 |
| SH15A 64.3 | Left trapezoid | Fragment | S2 |
| **Lower Limb** | | | |
| SH16 245.1 | Femur (unsided) | Femoral neck fragments | S2 |
| SH16 245.2 | Femur (unsided) | Femoral head fragments | S2 |
| SH16 271.1 | Femur (left) | Postero-lateral section of greater trochanter | S2 |
| SH16 238 | Femur (left) | Posterior section of diaphysis from sub-trochanteric region | 9A |
| SH15A 64.12 | Tibia (right) | Partial fragmented diaphysis and distal articular surface | 3, 9B |
| SH15A 64.13-15 | Fibula (right) | Partial fragmented diaphysis | 3 |
| SH15A 64.16 | Calcaneus (right) | Fragment of calcaneal tuberosity | S2 |
| SH15A 69.1 | Talus (right) | Complete | 3, 10A, S4 |

| | | | |
|---|---|---|---|
| SH15A 64.5 & SH15A 76.1 | Talus (left) | Medial process of left talus and part of subtalar facet | S2, S4 |
| SH15A 69.2 | Navicular (right) | Complete | 10B |
| SH15A 64.2 | Intermediate cuneiform (left) | Dorsal half | S2 |
| SH15A 64.10 | Lateral cuneiform (left) | Fragment | S2 |
| SH15A 64.8 | Fifth metatarsal (left) | Partial base | S2 |
| SH15A 64.9 | Metatarsal (unsided) | Head (possibly 2nd left) | S2 |
| SH16A 591 | Distal pedal phalanx (unsided) | Complete, probably ray 2 or 3 | 12 |

**Table 2**

Measurements of the SH16 269 adult thoracic vertebral body from Shanidar Cave

| Measurement | SH16 269 |
|---|---|
| Ventral cranio-caudal diameter (height) (M1) | 18.5 |
| Dorsal cranio-caudal diameter (height) (M2) | 19.7 |
| Median cranio-caudal diameter (height) (M3) | 15.7 |
| Superior dorso-ventral diameter (M4) | 19.5 |
| Inferior dorso-ventral diameter (M5) | 22.1 |
| Median dorso-ventral diameter (M6) | 20.2 |
| Superior transverse diameter (M7) | (26.0) |
| Inferior transverse diameter (M8) | 30.5 |
| Median transverse diameter (M9) | (26.8) |
| Maximum dorso-ventral diameter | 24.7 |
| Maximum transverse diameter | 30.3 |
| Maximum antero-posterior diameter excluding the anterior extension | 19.9 |
| Wedging of the vertebral body [a] | 0.1 |

Measurements in mm except wedging in degrees, following Trinkaus (1983) and Gómez-Olivencia et al. (2013) with Martin codes (Bräuer, 1988; Martin and Saller, 1957) given in parentheses and prefixed with 'M'. Definitions for other measurements can be found in Gómez-Olivencia et al. (2013).

Values in parentheses are estimated measurements.

[a] Calculated following Digiovanni et al. (1989).

**Table 3**

Measurements of the SH15 590 left hamate from Shanidar Cave, compared with other Shanidar Neanderthals and means for the Sima de los Huesos hominins, Neanderthals, Late Pleistocene *H. sapiens*, and recent *H. sapiens*. Data for samples given as mean ± standard deviation (sample size).

| **Measurement** | **SH15 590** | **Shanidar 3** [a] | **Shanidar 4** [a] | **Shanidar 5** [a] | **Sima de los Huesos** [b] | **Neanderthals** [c] | **Late Pleistocene *H. sapiens*** [d] | **Recent *H. sapiens*** [e] |
|---|---|---|---|---|---|---|---|---|
| **Side** | **L** | **R** | **L** | **R** | **—** | **—** | **—** | **—** |
| Articular length (M1) | 18.1 | (18.5) | 16.4 | 17.7 | 15.7 ± 0.7 (n = 4) | 17.9 ± 2.6 (n = 10) | 19.0 ± 3.0 (n = 16) | 17.1 ± 1.4 (n = 17) |
| Maximum breadth (M2) | 14.7 | | | | | 15.5 ± 1.0 (n = 4) | 15.2 ± 0.9 (n = 12) | 14.0 ± 1.7 (n = 17) |
| Maximum height (M3) | (22.1) | (28.5) | 28.2 | 25.2 | 22.7 ± 1.0 (n = 3) | 24.4 ± 3.0 (n = 8) | 21.1 ± 2.4 (n = 13) | 22.0 ± 1.7 (n = 17) |
| Body height (M4) | 11.4 | | | | | 13.3 (n = 1) | 12.6 ± 1.0 (n = 3) | 13.1 ± 1.1 (n = 17) |
| Hamulus projection (M5) | 10.7 | 13.6 | 12.9 | 10.9 | 10.4 ± 0.8 (n = 3) | 10.8 ± 2.0 (n = 6) | 7.8 ± 1.2 (n = 5) | 8.9 ± 1.2 (n = 17) |
| Articular height (M7) | 11.4 | | 13.6 | 11.1 | | 12.3 ± 1.7 (n = 2) | 10.1 ± 1.2 (n = 5) | 10.5 ± 0.8 (n = 17) |
| Articular breadth (M8) | 14.4 | | 15.3 | 15.3 | | 13.4 ± 2.1 (n = 4) | 14.8 ± 1.1 (n = 7) | 13.9 ± 1.6 (n = 17) |
| Maximum capitate articulation length (M9) | 16.6 | 10.9 | 16.7 | 17.7 | | 13.6 ± 3.3 (n = 5) | 15.7 ± 3.3 (n = 7) | 16.9 ± 1.3 (n = 17) |
| Maximum capitate articulation height (M10) | (10.2) | | 10.9 | 9.7 | | 10.3 ± 0.8 (n = 2) | 9.9 ± 1.5 (n = 6) | 10.4 ± 1.4 (n = 17) |
| Triquetral articulation length (M11) | 17.9 | | 17.7 | 17.9 | | 18.3 ± 0.8 (n = 3) | 15.1 ± 3.8 (n = 6) | 16.0 ±1.6 (n = 17) |
| Triquetral articulation height (M12) | (9.1) | | 9.2 | 9.2 | | 11 ± 3.1 (n = 3) | 10.0 ± 1.2 (n = 6) | 10.2 ± 1.3 (n = 17) |
| Hamulus length | 11.6 | 12.6 | 12.5 | 11.5 | 11.6 ± 0.3 (n = 3) | 10.7 ± 1.6 (n = 6) | 9.9 ± 2.1 (n = 8) | 10.0 ± 1.7 (n = 17) |
| Hamulus thickness | 6.3 | (6.3) | 7 | 6.5 | 5.3 ± 0.2 (n = 3) | 6.1 ± 0.5 (n = 6) | 4.7 ± 0.3 (n = 6) | 4.4 ± 0.7 (n = 17) |
| Hamulus projection index [f] | 48.4 | 47.7 | 45.7 | 43.3 | | 44.6 ± 1.7 (n = 8) | 37.1 ± 3.3 (n = 7) | 41.3 ± 2.4 (n = 17) |
| Hamulus cross-sectional area [g] | 73.1 | 79.4 | 87.5 | 74.8 | 62.1 ± 2.5 (n = 3) | 71.3 ± 17.0 (n = 9) | 52.5 ± 10.1 (n = 8) | 41.2 ± 11.2 (n = 17) |

Measurements in millimetres; hamulus cross-sectional area in $mm^2$. Martin codes (Bräuer, 1988; Martin and Saller, 1957) given in parentheses and prefixed with 'M'.

Values in parentheses are estimated measurements

[a] Data from Trinkaus (1983)

[b] Summary data from Lorenzo et al. (1999). Specimens: AT-939, AT-1310, AT-1311, AT-1313.

[c] Neanderthal sample: Amud 1 (Endo and Kimura, 1970; Trinkaus, 1983); Kebara 2 (Kivell et al., 2013); La Ferrassie 1 and 2 (Trinkaus, 1983); Palomas 96 (Walker et al., 2011); Regourdou 1 (Trinkaus, 1983); Shanidar 3, 4 and 5 (Trinkaus, 1983); and Tabun C1 and 3 (McCown and Keith, 1939).

[d] Late Pleistocene *H. sapiens* sample comprises: Abri Pataud 1 and 2 (Billy, 1975); Arancio 1 (Pardini and Lombardi Pardini, 1981); Chancelade 1 (Billy, 1969); Dolní Věstonice 3, 15 and 16 (Sládek et al., 2000); Minatogawa MB1 and MII♀1 (Baba and Endo, 1982); Nazlet Khater 2 (Crevecoeur, 2008); Qafzeh 3, 8 and 9 (Trinkaus, 1983; Vandermeersch, 1981); Skhul 4 and 5 (McCown and Keith, 1939); Sunghir 1 (Trinkaus et al., 2014); Tagliente 1 (Corrain, 1977); Tianyuan (Shang and Trinkaus, 2010).

[e] This study, collected by MML. See Supplementary Information for sample details.

[f] Hamulus projection index = (Hamulus projection/Maximum height)*100.

[g] Hamulus cross-sectional area = Hamulus length * Hamulus thickness.

**Table 4**

Measurements of the SH15A 69.1 talus from Shanidar Cave, compared with mean values from the Sima de los Huesos hominins, Neanderthals, Middle Pleistocene *Homo* from Jinniushan and Omo Kibish, Late Pleistocene *H. sapiens* and recent *H. sapiens.* Data given as mean ± standard deviation (sample size).

| **Measurement** | **SH15A 69.1** | **Sima de los Huesos** [a] | **Neanderthals** [b] | **Jinniushan 1 (right)** [c] | **Omo 1 (KHS 1-59) (right)** [d] | **Late Pleistocene *H. sapiens*** [e] | **Recent *H. sapiens*** [a] |
|---|---|---|---|---|---|---|---|
| Talar length (M1) | 48.3 | 51.9 ± 3.5 (n = 18) | 51.2 ± 3.5 (n = 21) | | (53.8) | 52.6 ± 4.2 (n = 36) | 52.8 ± 4.0 (n = 162) |
| Total length (M1a) | 51.6 | 55.4 ± 4.0 (n = 16) | 55.0 ± 4.0 (n = 22) | | | 57.6 ± 4.5 (n = 25) | 57.5 ± 4.7 (n = 162) |
| Total breadth (M2) | 43.0 | 41.8 ± 3.2 (n = 18) | 44.5 ± 4.9 (n = 21) | | 43.1 | 43.7 ± 3.8 (n = 29) | 41.1 ± 3.6 (n = 162) |
| Articular breadth (M2b) | 42.9 | 40.9 ± 3.2 (n = 20) | 43.7 ± 4.4 (n = 20) | | | 44.0 ± 4.3 (n = 21) | 41.1 ± 3.9 (n = 162) |
| Talar height (M3) | 29.7 | 28.9 ± 2.4 (n = 18) | 31.4 ± 3.3 (n = 16) | | 27.5 | 30.9 ± 2.8 (n = 29) | 29.0 ± 4.0 (n = 112) |
| Medial height (M3-1) | 31.8 | 30.3 ± 2.7 (n = 17) | 32.9 ± 3.1 (n = 19) | | | 33.1 ± 3.0 (n = 18) | 31.5 ± 2.7 (n = 162) |
| Trochlear length (M4) | 34.3 | 33.3 ± 2.6 (n = 19) | 33.3 ± 3.3 (n = 24) | 36.5 | 26.2 | 33.9 ± 3.3 (n = 36) | 33.1 ± 2.9 (n = 162) |
| Trochlear breadth (M5) | 30.1 | 29.1 ± 2.3 (n = 20) | 28.6 ± 2.1 (n = 22) | 30.3 | (25.3) | 29.3 ± 2.7 (n = 36) | 29.0 ± 2.5 (n = 162) |
| Posterior trochlear breadth (M5-1) | (26.3) | 27.0 ± 2.2 (n = 18) | 26.2 ± 3.0 (n = 19) | | (21.3) | 24.2 ± 2.8 (n = 20) | 26.1 ± 2.6 (n = 112) |
| Anterior trochlear breadth (M5-2) | (29.8) | 30.2 ± 2.5 (n = 19) | 29.6 ± 3.1 (n = 19) | | | 30.5 ± 2.8 (n = 20) | 30.3 ± 2.5 (n = 112) |
| Trochlear height (M6) | 13.2 | 9.1 ± 1.0 (n = 18) | 9.5 ± 1.3 (n = 22) | | | 10.1 ± 1.4 (n = 20) | 8.4 ± 1.0 (n = 162) |
| Lateral malleolar oblique height (M7) | 27.2 | 24.9 ± 1.5 (n = 20) | 25.5 ± 3.3 (n = 24) | | | 25.5 ± 2.7 (n = 16) | 23.7 ± 2.4 (n = 162) |
| Lateral malleolar breadth (M7a) | 9.8 | 13.2 ± 2.0 (n = 20) | 10.7 ± 2.5 (n = 24) | | | 10.3 ± 1.3 (n = 16) | 9.4 ± 2.2 (n = 112) |
| Head-neck length (M8) | 20.2 | 20.5 ± 1.9 (n = 18) | 19.0 ± 2.1 (n = 23) | | 20.3 | 20.7 ± 3.7 (n = 26) | 23.1 ± 2.9 (n = 112) |
| Length of the head (M9) | 35.6 | 30.4 ± 2.2 (n = 18) | 34.7 ± 3.4 (n = 23) | | (30.1) | 33.5 ± 2.9 (n = 26) | 32.5 ± 2.9 (n = 161) |
| Breadth of the head (M10) | 24.1 | 21.8 ± 1.9 (n = 18) | 22.5 ± 2.2 (n = 24) | 31.3 | (19.8) | 22.0 ± 2.5 (n = 26) | 22.3 ± 2.2 (n = 162) |

| | | | | | | | |
|---|---|---|---|---|---|---|---|
| Length of the calcaneal posterior articular surface (M12) | 30.8 | 31.3 ± 1.9 (n = 17) | 32.0 ± 3.2 (n = 21) | 21.5 | (3.4) | 32.7 ± 3.3 (n = 24) | 31.2 ± 2.7 (n = 162) |
| Breadth of the calcaneal posterior articular surface (M13) | 21.9 | 21.6 ± 1.6 (n = 20) | 22.2 ± 1.6 (n = 23) | | 20.3 | 22.4 ± 2.3 (n = 26) | 21.5 ± 2.1 (n = 162) |
| Depth of the calcaneal posterior articular surface (M14) | 5.5 | 8.1 ± 1.3 (n = 19) | 7.4 ± 1.6 (n = 15) | | | 6.5 ± 2.1 (n = 11) | 8.0 ± 1.8 (n = 162) |
| Trochlear depth | 0.4 | 1.1 ± 0.2 (n = 19) | 1.2 ± 0.4 (n = 16) | | | 1.1 ± 0.3 (n = 7) | 1.7 ± 0.4 (n = 112) |
| Lateral malleolar length | (29.3) | 32.1 ± 2.3 (n = 20) | 31.8 ± 3.5 (n = 20) | | | 31.0 ± 2.9 (n = 9) | 31.8 ± 2.8 (n = 112) |
| Length of the calcaneal middle articular surface | 18.1 | 20.2 ± 2.6 (n = 13) | 19.8 ± 3.3 (n = 11) | | | 22.9 ± 1.4 (n = 3) | 22.0 ± 3.7 (n = 111) |
| Breadth of the calcaneal middle articular surface | 13.8 | 14.5 ± 2.3 (n = 17) | 15.0 ± 1.6 (n = 14) | | | 15.5 ± 1.0 (n = 6) | 13.6 ± 1.7 (n = 111) |
| Lateral height | 28.9 | 28.9 ± 2.3 (n = 20) | 31.1 ± 3.0 (n = 16) | | | 31.4 ± 1.1 (n = 4) | 29.7 ± 4.1 (n = 112) |
| Medial malleolar length | 31.9 | 31.1 ± 2.4 (n = 15) | 30.2 ± 3.7 (n = 17) | | | 31.8 ± 2.6 (n = 7) | 31.1 ± 3.0 (n = 112) |
| Sulcus tali breadth | 7.0 | 4.7 ± 1.0 (n = 18) | 5.5 ± 1.1 (n = 14) | | | 5.3 ± 1.0 (n = 4) | 5.6 ± 1.3 (n = 112) |
| Lateral malleolar height | 27.0 | 22.7 ± 1.5 (n = 20) | 23.9 ± 3.0 (n = 24) | | | 24.9 ± 3.4 (n = 12) | 22.6 ± 2.4 (n = 112) |
| Head-neck length/trochlea length ratio ((M8/M3) * 100) | 59.0 | | 57.6 ± 6.1 (n = 18) | | 77.5 | 62.2 ± 11.0 (n = 26) | 62.6 ± 5.2 (n = 50) [f] |

Measurements in mm, following Trinkaus (1975a, 1983b) and Pablos et al. (2013b) with Martin codes (Bräuer, 1988; Martin and Saller, 1957) given in parentheses and prefixed with 'M'. Definitions for other measurements can be found in Pablos et al. (2013b).

Values in parentheses for SH15A 69.1 and Omo 1 are estimated measurements.

[a] Data from Pablos et al. (2013b).

[b] Neanderthal sample from Pablos et al. (2013b), comprising: Amud 1; Kiik-Koba 1; Krapina 235, 236, 237, 238, 238.1, 238.2 and 238.7, 238.3, 238.4, 238.5, 238.6, 239.1, 239.2; La Chapelle 1; La Ferrassie 1 and 2; La Quina 1; Regourdou 1; Shanidar 1 and 3; Spy 2; and Tabun C1. See Pablos et al. (2013b) for details on sources of data.

[c] Lu et al. (2011).

[d] Pearson et al. (2008).

[e] Late Pleistocene *H. sapiens* sample comprises: Abri Pataud 1 (A. Pablos, pers. comm. February 2017); Arene Candide 2, 4, 5, 10 and 13 (Paoli et al., 1980); Arancio 1 (Pardini and Lombardi Pardini, 1981); Cap Blanc 1 (Billy 1975); Chancelade 1 (Billy, 1969); Cro-magnon 4337 and 4338 (A. Pablos, pers. comm. February 2017); Dolní Věstonice 3, 13, 15 and 16 (Sládek et al., 2000); El Mirón 1 (Carretero et al., 2015);

Gough's Cave 1.1/29 and 89 67 (A. Pablos, pers. comm. February 2017); Grotte des Enfants 1 and 2 (Fraipont, 1913); Le Peyrat 5 (Patte, 1968); Minatogawa 1 and 2 (Baba and Endo, 1982); Mladeč 30 (Trinkaus et al., 2006); Paviland 1 (Q1/16) (Trinkaus, 2000);; Předmostí 3, 9, 10 and 14 (Matiegka, 1938); Qafzeh 3, 8 and 9 (Vandermeersch, 1981); Skhul 4, 5, 6, and 7 (McCown and Keith, 2939); Sunghir 1 (Trinkaus et al., 2014); Tagliente 1 (Corrain, 1977); and Tianyuan 1 (Shang and Trinkaus, 2010).

[f] Data from Trinkaus (1983) for recent Europeans.

**Table 5**

Measurements of the SH15A 69.2 right navicular from Shanidar Cave compared with mean values from the Sima de los Huesos hominins, Neanderthals, Middle Pleistocene *Homo* from Jinniushan and Omo Kibish, Late Pleistocene *H. sapiens* and recent *H. sapiens*. Data given as mean ± standard deviation (sample size).

| **Measurement** | **SH15A 69.2** | **Sima de los Huesos** [a] | **Neanderthals** [b] | **Jinniushan 1 (right)** [c] | **Omo 1 (KHS 1-45) (right)** [d] | **Late Pleistocene *H. sapiens*** [e] | **Holocene *H. sapiens*** [f] |
|---|---|---|---|---|---|---|---|
| Breadth (M1) | 44.1 | 44.2 ± 4.0 (n = 9) | 43.8 ± 3.4 (n = 11) | 40.3 | 37.8 | 39.1 ± 3.4 (n = 27) | 40.3 |
| Height (M2) | 27.5 | | 28.2 ± 2.5 (n = 11) | 24.3 | 25.7 | 27.4 ± 2.9 (n = 27) | 26.8 |
| Talar articular length (M3) | 29.1 | | 29.6 ± 1.7 (n = 11) | | 28.5 | 27.0 ± 2.7 (n = 21) | 28.0 |
| Talar articular height (M4) | 22.3 | | 22.2 ± 1.8 (n = 11) | | 21.5 | 21.5 ± 2.2 (n = 21) | 21.7 |
| Cuneiform articular length (M6) | 34.7 | | 36.0 ± 4.4 (n = 5) | | 36.7 | 34.5 ± 2.2 (n = 11) | |
| Minimum thickness (M7) | 7.7 | | 8.1 ± 1.0 (n = 13) | | 9.0 | 9.0 ± 1.2 (n = 27) | 9.5 |
| Maximum thickness (M8) | 22.6 | | 21.6 ± 1.3 (n = 9) | | 14.0 | 18.6 ± 1.4 (n = 24) | 19.4 |
| Tuberosity length | 12.8 | | 10.7 ± 1.2 (n = 10) | 13.1 | | 9.3 ± 2.3 (n = 6) | 10.1 |
| Tuberosity thickness | 23.4 | | 23.1 ± 1.5 (n = 10) | | | 17.2 ± 0.2 (n = 3) | 18.2 |
| Wedging index [g] | 34.2 | | 37.0 ± 4.2 (n = 9) | | 49.2 | 48.5 ± 6.0 (n = 22) | 49.2 |
| Tuberosity thickness index [h] | 302.9 | | 292.5 ± 35.3 (n = 10) | | | 134.8 ± 117.9 (n = 3) | 191.6 |

Measurements in mm, following Trinkaus (1975a, 1983b) with Martin codes (Bräuer, 1988; Martin and Saller, 1957) given in parentheses and prefixed with 'M'.

[a] Data from Pablos et al. (2017a).

[b] Neanderthal sample: Amud 1 (Endo and Kimura, 1970); Kiik-Koba 1 (Trinkaus, 1975); Kalamakia 14 (Harvati et al., 2013); Krapina 241 and 242 (Trinkaus, 1975); La Ferrassie 1 and 2 (Trinkaus, 1975); Moula-Guercy M-G2-464 and M-S-18 (Mersey et al., 2013); Shanidar 1, 3 and 4 (Trinkaus, 1983); and Tabun C1 (Trinkaus, 1983).

[c] Lu et al. (2011).

[d] Pearson et al. (2008).

[e] Late Pleistocene *H. sapiens* sample comprises: Abri Pataud 1 (A. Pablos, pers. comm. February 2017); Arene Candide 2, 3, 4, 5 and 10 (Paoli et al., 1980); Cap Blanc 1 (Billy, 1975); Chancelade 1 (Billy, 1969); Cro-Magnon 4340 and 4339 (A. Pablos, pers. comm. February 2017); Cueva de los Torrejones (Pablos et al., 2017b); Dolní Věstonice 15, 16 and 39 (Sládek et al., 2000); El Mirón 1 (Carretero et al., 2015); Le Peyrat 5 (Patte, 1968); Minatogawa 3 (Baba and Endo, 1982); Paviland 1 (Trinkaus, 2000);; Predmostí 3, 9, 10 and 14 (Matiegka, 1938); Qafzeh 3, 8 and 9 (Vandermeersch, 1981); Skhul 4 and 6 (Trinkaus, 1975); Sunghir 1 (Trinkaus et al., 2014); and Tagliente 1 (Corrain, 1977).

[f] Data from Harvati et al. (2013). N = 20, including individuals from medieval German, Masai, and Tunisian populations from the Paleoanthropology osteological collections, University of Tübingen.

[g] Wedging index = 100*(Minimum thickness/Maximum thickness).

[h] Tuberosity thickness index =100*(Tuberosity thickness/Minimum thickness) (Trinkaus, 1983).

**Table 6**

Measurements of the SH15A 64.2 left intermediate cuneiform from Shanidar Cave compared with mean values from the Sima de los Huesos hominins, Neanderthals, Late Pleistocene *H. sapiens* and recent *H. sapiens*. Data given as mean ± standard deviation (sample size).

| **Measurement** | **SH15A 64.2** | **Sima de los Huesos** [a] | **Neanderthals** [b] | **Late Pleistocene *H. sapiens*** [c] | **Holocene *H. sapiens*** |
|---|---|---|---|---|---|
| Superior length (M1) | 17.1 | 15.4 ± 0.9 (n = 12) | 16.8 ± 1.1 (n = 9) | 16.9 ± 2.0 (n = 19) | 17.5 ± 1.7 (n = 112) [d] |
| Middle length (M2) | | | 15.3 ± 0.6 (n = 3) | 15.6 ± 1.4 (n = 18) | |
| Mean articular length | | | 15.9 ± 0.9 (n = 6) | 15.3 (n = 1) | 16.2 ± 1.0 (n = 40) [e] |
| Proximal articular height | | | 19.3 ± 1.9 (n = 6) | 19.3 ± 2.4 (n = 3) | |
| Proximal articular breadth (M4) | 15.45 | | 15.2 ± 1.2 (n = 7) | 14.9 ± 1.8 (n = 14) | |
| Distal articular height | | | 19.6 ± 2.5 (n = 6) | 21.2 ± 1.1 (n = 4) | |
| Distal articular breadth (M3) | 15.22 | | 14.9 ± 1.4 (n = 9) | 13.6 ± 1.9 (n = 13) | |

Measurements in mm, following Trinkaus (1975a, 1983b) with Martin codes (Bräuer, 1988; Martin and Saller, 1957) given in parentheses and prefixed with 'M'.

[a] Data from Pablos et al. (2017a).

[b] Neanderthal sample: Amud 1 (Endo and Kimura, 1970); Kiik-Koba 1 (Trinkaus, 1975); La Ferrassie 1 and 2 (Trinkaus, 1975); Shanidar 1, 3, 4 and 6 (Trinkaus, 1983); and Tabun C1 (McCown and Keith, 1939).

[c] Lu et al. (2011).

[d] Pearson et al. (2008).

[e] Late Pleistocene *H. sapiens* sample comprises: Abri Pataud 1 (Billy, 1975); Arene Candide 1, 4, 5 and 10 (Paoli et al., 1980); Chancelade 1 (Billy, 1969); Dolní Věstonice 3 and 16 (Sládek et al., 2000); El Mirón 1 (Carretero et al., 2015); Predmostí 3, 9, 10 and 14 (Matiegka, 1938); Qafzeh 3, 8 and 9 (Vandermeersch, 1981); Skhul 4 (McCown and Keith, 1939; Trinkaus, 1975); Sunghir 1 (Trinkaus et al., 2014); and Tagliente 1 (Corrain, 1977).

**Table 7**

Measurements of the SH15A 64.9 adult metatarsal head from Shanidar Cave

| Measurement | SH15A 64.9 |
|---|---|
| Distal epiphyseal breadth | 14.3 |
| Distal articular breadth (M8b) | 12.3 |
| Distal articular height (M9a) | (15.8) |

Measurements in mm, following Pablos et al. (2012) with Martin codes (Bräuer, 1988; Martin and Saller, 1957) given in parentheses and prefixed with 'M'

Values in parentheses are estimated measurements.

**Table 8**

Measurements of the adult distal pedal phalanx (SH16A 591) and other distal pedal phalanges from Shanidar Cave.

| **Measurement** | **SH16A 591** | **Shanidar 6 [a]** | **Shanidar 4 [a]** | | | | | |
|---|---|---|---|---|---|---|---|---|
| **Ray** | **?2** | **1** | **1** | **?2** | **?2** | **?3** | **?4** | **?5** |
| **Side** | **?** | **R** | **L** | **?** | **?** | **?** | **?** | **?** |
| Maximum length [b] | 14.3 | | | | | | | |
| Articular length (M1) | 12.6 | | (27.0–27.5) | 11.2 | 11.2 | 11.1 | 10.5 | 8.7 |
| Midshaft breadth (M2) | 6.3 | | | 6.6 | 6.1 | 6 | 6.8 | 5.6 |
| Midshaft height (M3) | 6.0 | | | 5.9 | 5.8 | 5.8 | 6 | 5.7 |
| Proximal maximum height | 8.1 | 9.2 | 11.9 | 7.3 | 7.8 | 7.6 | 6.8 | 7.4 |
| Proximal maximum breadth | (13.0)[c] | (19.0) | (21.5) | 12 | 11.8 | 11.1 | 10.9 | 10.4 |
| Proximal articular height | 6.8 | 7 | 9.5 | 4.6 | 4.5 | 5 | 4.1 | 5.3 |
| Proximal articular breadth | 9.4 | (16.4) | (15.0) | 9.2 | 8.2 | 7.6 | 9.2 | 8.0 |
| Distal height | 5.4 | | 8.3 | 4.2 | 5.3 | 5.3 | 5.5 | 4.9 |
| Distal breadth | 10.4 | (12.0) | 15.4 | 10.3 | 8.8 | 8.4 | 9.6 | 7.7 |

Measurements in mm, following Trinkaus (1975a, 1983b) with Martin codes (Bräuer, 1988; Martin and Saller, 1957) given in parentheses where relevant.

Values in parentheses are estimated measurements.

[a] Measurements of Shanidar 4 and 6 from Trinkaus (1983).

[b] Maximum length follows White, Black and Folkens (2011). Measurements in parentheses are estimated.

[c] Excluding osteophytes.

**Supplementary Online Material:**

# Newly-discovered Neanderthal remains from Shanidar Cave, Iraqi Kurdistan, and their attribution to Shanidar 5

Emma Pomeroy [a,*], Marta Mirazón Lahr [b], Federica Crivellaro [c], Lucy Farr [d], Tim Reynolds [e], Chris O. Hunt [f], Graeme Barker [g]

[a] School of Natural Sciences and Psychology, Liverpool John Moores University, James Parsons Building, Byrom Street, Liverpool L3 3AF, UK. Email: E.E.Pomeroy@ljmu.ac.uk

[b] Leverhulme Centre for Human Evolutionary Studies, Department of Archaeology and Anthropology, University of Cambridge, Fitzwilliam Street, Cambridge CB2 1QH, UK. Email: mbml1@cam.ac.uk

[c] Leverhulme Centre for Human Evolutionary Studies, Department of Archaeology and Anthropology, University of Cambridge, Fitzwilliam Street, Cambridge CB2 1QH, UK. Email: fc285@cam.ac.uk

[d] McDonald Institute for Archaeological Research, University of Cambridge, Downing Street, Cambridge CB2 3ER, UK. Email: lrf24@cam.ac.uk

[e] Department of History, Classics & Archaeology, Birkbeck College, University of London, Russell Square, London WC1B 5DQ, UK. Email: te.reynolds@bbk.ac.uk

[f] School of Natural Sciences and Psychology, Liverpool John Moores University, James Parsons Building, Byrom Street, Liverpool L3 3AF, UK. Email: C.O.Hunt@ljmu.ac.uk

[g] McDonald Institute for Archaeological Research, University of Cambridge, Downing Street, Cambridge CB2 3ER, UK. Email: gb314@cam.ac.uk

**Figure S1.** Views of the 1960 and 2015-6 excavations at Shanidar Cave (arrows). Left: View of Ralph Solecki's excavations at Shanidar Cave illustrating the location of the Shanidar 5 finds. Right: 2015–2016 excavations showing the location of remains described in this paper. (1960 photograph with kind permission of Ralph Solecki).

**Figure S2.** Smaller fragments attributed to Shanidar 5 described in the text. Scale bars = 10 mm. See Table 1 for further details.

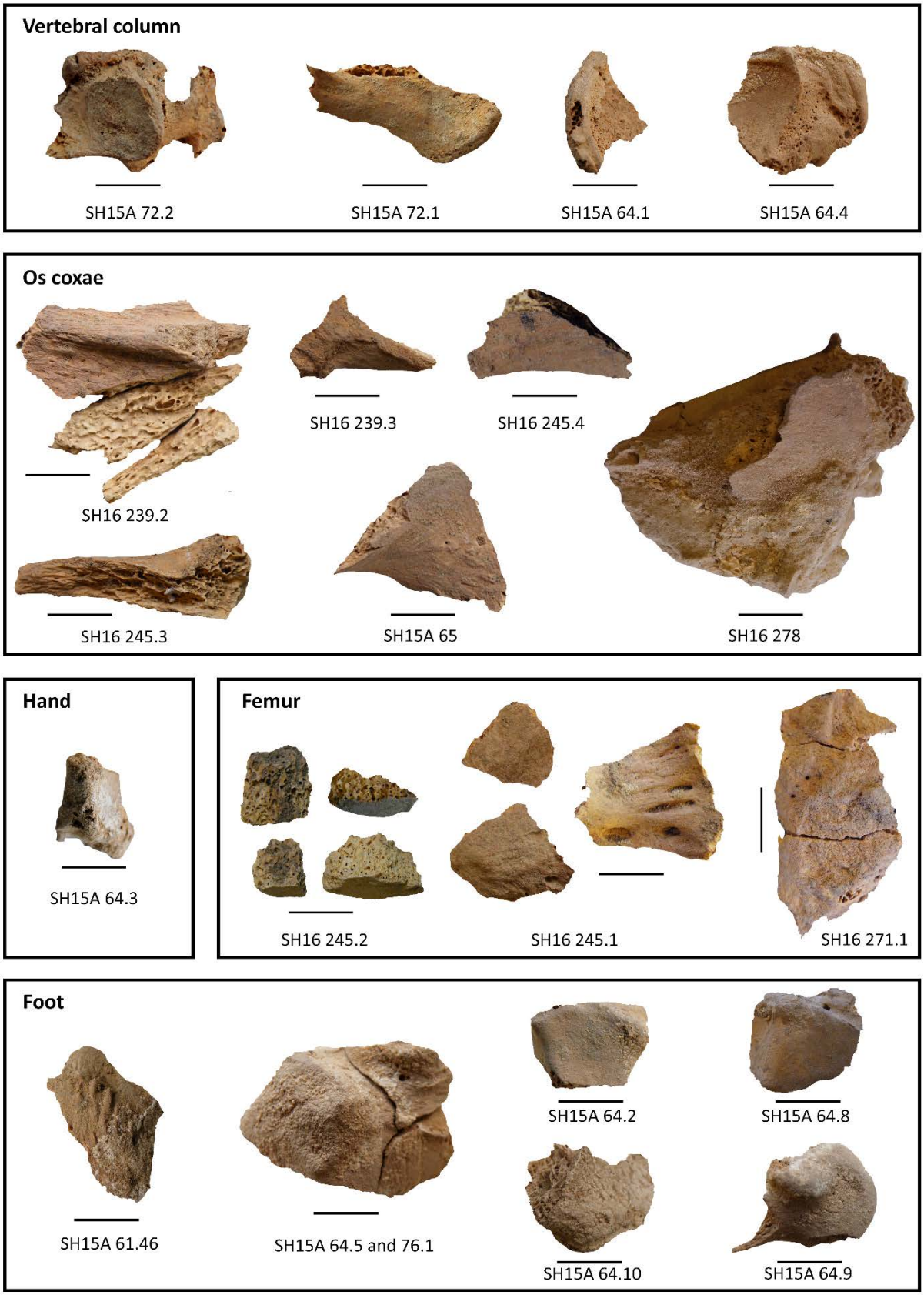

**Text S1**

**The SH15 590 adult left hamate**

To assess the taxonomic affinities of SH15 590, comparative data were collected by MML from recent *H. sapiens* specimens from the Duckworth Collection, University of Cambridge, representing a broad geographic range (Table S1). Comparative data from the literature on Neanderthals and *H. sapiens* were also gathered from the literature (see footnotes to main text Table 3 for references).

**Table S1**

Hamate specimens from the Duckworth Collection, University of Cambridge, used in this study.

| Individual | Side | Provenance |
|---|---|---|
| Am.15.1.22 | L | Kechipawan site, New Mexico, USA. Sedentary Pueblo, farming community, dating to the late Protohistoric-early Colonial period. |
| Am.15.1.25 | L & R | Kechipawan site, New Mexico, USA. Sedentary Pueblo, farming community, dating to the late Protohistoric-early Colonial period. |
| Esk II | R | Eskimo from Greenland; ethnographic. Arctic hunters and coastal foragers |
| Am.1.o.10 | R | Eskimo from Ungava Bay, NE Canada. Arctic hunters and coastal foragers |
| Mor3734/45 | L | Moriori, New Zealand; ethnographic. |
| Aus001 | L | Australian Aboriginal; ethnographic. |
| Aus015 | L & R | Australian Aboriginal; ethnographic. |
| And17 | L & R | Andaman Islander; ethnographic |
| NU547/SK517 | L | Nubian; ancient Nile Valley |
| NU551/SK566 | L | Nubian; ancient Nile Valley |
| AF1736 | L & R | Jebel Moya, 1st millennium BC Sudanese Nile Valley. Semi-sedentary pastoralists |
| AF1741 | L & R | Jebel Moya, 1st millennium BC Sudanese Nile Valley. Semi-sedentary pastoralists |

**Bilateral asymmetry and the attribution of the SH15 590 hamate to previously-reported individuals from Shanidar Cave**

Among the adult Neanderthal remains from the earlier excavations at Shanidar, there are three hamate bones—two right hamates from Shanidar 3 and Shanidar 5, and a left hamate from Shanidar 4 (Stewart, 1977; Trinkaus, 1982, 1983). All three are complete or substantially complete, and show the distinctive Neanderthal features (Trinkaus, 1983). The new Shanidar Neanderthal left hamate could originate from a new adult Neanderthal in the cave, or from Shanidar 3 or Shanidar 5 (the two Shanidar adults with preserved right hamates). Adult left and right hands of the same individual are normally asymmetrical, especially among right-handed people, whose right hand is noticeably larger than the left (Purves et al., 1994). Furthermore, this bilateral asymmetry is not expressed equally throughout the wrist and hand bones. Therefore, to assess whether the new Shanidar hamate could belong to the left hand of Shanidar 3 or 5, the degree of bilateral asymmetry in hamate dimensions was estimated on six modern human hands, which include hunter-gatherers, semi-nomadic pastoralists and a traditional agriculturalist (Table S2). The results offer a measure of likelihood, since the data for the Shanidar 3 right hamate is partial, the new Shanidar hamate is incomplete (affecting in particular estimates of its height), and the bilateral modern sample is small. However, the analysis offers a useful indication.

Table S2 shows the differences in hamate dimensions between the new Shanidar left hamate and both the Shanidar 3 and Shanidar 5 right hamates (first two columns), as well as the bilateral differences between left and right hamates in modern humans (the directionality of the difference—i.e., whether the left or the right bone was larger, is ignored). In the six left-right pairs of modern human hamates, there is an average difference of 0.5 mm, ranging from 0.2–0.7 mm. Among individual dimensions, the range of left-right asymmetry varied from a minimum of 0.1 mm

(hamulus thickness) to a maximum of 0.8 mm (triquetral articular length). Large bilateral differences were also observed in the maximum height of the hamate.

The mean difference between the SH15 590 left hamate and the right hamate from Shanidar 3 is six times greater than the human left-right average (Table S2). The differences are also larger for almost all dimensions than those observed between the SH15 590 left hamate and the right hamate from Shanidar 5. The latter are within the parameters of asymmetry between modern human left and right hamates. The largest difference observed from both the Shanidar 3 and Shanidar 5 right hamates was for height, which could reflect an inaccurate measurement of the SH15 590 hamate because of the missing fragment. Removing this variable from the calculations, however, does not change the pattern of similarity, and the similarities between the new left Shanidar hamate and the right hamate from Shanidar 5 (0.4 mm) remain within the modern human range. Therefore, while it is not possible to prove that the SH15 590 hamate belongs to the left hand of Shanidar 5, its dimensions are consistent with this scenario. The SH15 590 left hamate is compared with the original Shanidar 5 right hamate in Figure S3.

**Table S2**

Differences between the new left SH15 590 hamate and the right hamates from Shanidar 3 and Shanidar 5, compared with differences between the left and right hamates of six modern humans.

| Measurement | SH15 590 - Sh3 | SH15 590 - Sh5 | Sung1 | Kech25 | Aus15 | And17 | JB1736 | JB1741 |
|---|---|---|---|---|---|---|---|---|
| Maximum height (M3) | **0.4** | **0.4** | 0.4 | 0.2 | 0.6 | 0.4 | 0.2 | 0.5 |
| Body height (M4) | **6.4** | **3.1** | 0.9 | 0.2 | 0.3 | 1.6 | 0.7 | 0.0 |
| Hamulus projection (M5) | **2.9** | **0.2** | 0.5 | 0.1 | 0.5 | 0.1 | 0.5 | 0.7 |
| Articular height (M7) | | **0.3** | | 0.0 | 0.3 | 0.8 | 0.1 | 0.0 |
| Articular breadth (M8) | | **0.9** | 0.9 | 0.2 | 0.0 | 0.3 | 0.5 | 1.0 |
| Maximum capitate articulation length (M9) | **5.7** | **1.1** | 0.9 | 0.3 | 0.1 | 0.3 | 0.3 | 0.7 |
| Maximum capitate articulation height (M10) | | **0.5** | 0.3 | 0.4 | 1.4 | 0.1 | 0.5 | 0.4 |
| Triquetral articulation length (M11) | | **0.0** | | 0.4 | 3.1 | 0.2 | 0.2 | 0.2 |
| Triquetral articulation height (M12) | | **0.1** | | 0.5 | 0.5 | 0.9 | 0.0 | 0.7 |
| Hamulus length | **1.0** | **0.1** | 0.8 | 0.3 | 0.3 | 0.0 | 0.1 | 0.5 |
| Hamulus thickness | **0.0** | **0.2** | 0.1 | 0.0 | 0.1 | 0.2 | 0.3 | 0.1 |
| **Mean** | **2.7** | **0.6** | **0.6** | **0.2** | **0.7** | **0.5** | **0.3** | **0.4** |
| **Mean (excluding M3)** | **2.0** | **0.4** | **0.6** | **0.2** | **0.7** | **0.3** | **0.3** | **0.5** |

The modern humans are: Siberian Upper Palaeolithic individual Sunghir 1 (Trinkaus et al., 2014) and the following specimens from the Duckworth Collection, University of Cambridge: native American, New Mexico (Kech25); Australian Aborigine (Aus15); Andaman Islander (And17); and two individuals from the 1st millennium BC Sudanese site of Jebel Moya (JB1736 and JB1741). Measurements in mm.


**Figure S3.** Comparison of the SH15 590 left hamate with the original Shanidar 5 right hamate. Scale bar = 10 mm. (Photographs of Shanidar 5 right hamate courtesy of Erik Trinkaus).

**Figure S4.** Comparison of recently-discovered fragment of the subtalar facet of the left talus (SH15A 64.5) with the same region of the right talus (SH15A 69.1) from Shanidar Cave. Scale bar = 10 mm.

**Table S3.**

Stature estimates from talar measurements using equations from Will and Stock (2015).

| Talus measurement | | | Stature estimation equation (Will and Stock 2015) | | | | Estimated stature (cm) |
|---|---|---|---|---|---|---|---|
| Will and Stock (2015) code | Martin code | SH15A 69.1 (mm) | Equation | $R^2$ | p | %SEE | |
| Ta6 | 1b | 51.6 | 0.728 + (1.371 * Ta6 ) | 0.73 | <0.01 | 2.5 | 156.0 |
| Ta8 | M9 | 35.6 | 0.678 + (1.579 * Ta8 ) | 0.68 | <0.01 | 2.8 | 170.0 |
| Ta12 | M5 | 30.1 | 0.619 + (1.497 * Ta12 ) | 0.62 | <0.01 | 3.1 | 164.8 |
| Ta19 | M13 | 21.9 | 0.591 + (1.723 * Ta19 ) | 0.59 | <0.01 | 3.2 | 163.0 |
| Ta11 | M4 | 34.3 | 0.242 + (1.669 * Ta11 ) | 0.24 | <0.05 | 4.4 | 162.0 |
| Ta18 | M12 | 30.8 | 0.164 + (1.843 * Ta18 ) | 0.16 | n.s. | 4.5 | 159.7 |

Details of the equations are from Will and Stock (2015: SOM Table 8). Equations given in order of reported percent standard error of estimate (%SEE). Note that the equations from Will and Stock (2015) are for log-transformed data.

**Table S4**

Body mass estimates from talar measurements using equations from Will and Stock (2015) to estimate femoral head diameter, and equations from Ruff et al. (1991), McHenry (1992) and Grine et al. (1995) to then estimate body mass.

| Talus measurement | | | Femoral head diameter estimation equation (Will and Stock 2015) | | | | Estimated femoral head diameter | Body mass estimates (kg) | | | |
|---|---|---|---|---|---|---|---|---|---|---|---|
| Will and Stock (2015) code | Martin code | SH15A 69.1 (mm) | Equation | $R^2$ | p | %SEE | (mm) | Ruff et al. (1991) | McHenry (1992) | Grine et al. (1995) | Mean estimate [a] |
| Ta8 | M9 | 35.6 | 0.672 + (0.648* Ta8) | 0.66 | <0.01 | 4.6 | 47.6 | 70.2 | - | 71.4 | 70.6 |
| Ta6 | 1b | 51.6 | 0.558 + (0.619 * Ta6) | 0.56 | <0.01 | 4.9 | 41.5 | 58.4 | 53.0 | 57.6 | 56.3 |
| Ta12 | M5 | 30.1 | 0.64 + (0.686 * Ta12) | 0.50 | <0.01 | 5.6 | 45.1 | 65.4 | 61.1 | 65.8 | 64.1 |
| Ta18 | M12 | 30.8 | 0.842 + (0.532 * Ta18) | 0.35 | <0.05 | 6.0 | 43.0 | 61.4 | 56.5 | 61.1 | 59.7 |
| Ta19 | M13 | 21.9 | 1.05 + (0.444 * Ta19) | 0.40 | <0.01 | 6.2 | 44.2 | 63.5 | 59.0 | 63.7 | 62.1 |
| Ta11 | M4 | 34.3 | 0.697 + (0.617 * Ta11) | 0.30 | <0.05 | 6.7 | 44.1 | 63.4 | 58.8 | 63.5 | 61.9 |

Details of the equations are from Will and Stock (2015: SOM Table 9). Equations given in order of reported percent standard error of estimate (%SEE). Note that the equations from Will and Stock (2015) are for log-transformed data.

[a] Following Ruff (2010), for femoral head diameters > 47 mm, the mean of the Ruff et al. (1991) and Grine et al. (1995) equations was used, while for femoral head diameters ≤47mm, the mean of Ruff et al. (1991), McHenry (1992) and Grine et al. (1995) was used.

**Supplementary references**


Grine, F.E., Jungers, W.L., Tobias, P.V., Pearson, O.M., 1995. Fossil *Homo* femur from Berg Aukas, northern Namibia. Am. J. Phys. Anthropol. 97, 151–185.

McHenry, H.M., 1992. Body size and proportions in early hominids. Am. J. Phys. Anthropol. 87, 407–431.

Purves, D., White, L.E., Andrews, T.J., 1994. Manual asymmetry and handedness. Proc. Natl. Acad. Sci. 91, 5030–5032.

Ruff, C.B., 2010. Body size and body shape in early hominins - implications of the Gona Pelvis. J. Hum. Evol. 58, 166–178.

Ruff, C.B., Scott, W.W., Liu, A.Y., 1991. Articular and diaphyseal remodeling of the proximal femur with changes in body mass in adults. Am. J. Phys. Anthropol. 86, 397–413.

Stewart, T.D., 1977. The Neanderthal Skeletal Remains from Shanidar Cave, Iraq: A Summary of Findings to Date. Proc. Am. Philos. Soc. 121, 121–165.

Trinkaus, E., 1982. The Shanidar 3 Neandertal. Am. J. Phys. Anthropol. 57, 37–60.

Trinkaus, E., 1983. The Shanidar Neandertals. Academic Press, New York.

Trinkaus, E., Buzhilova, A.P., Mednikova, M.B., Dobrovolskaya, M.V., 2014. The People of Sunghir: Burials, Bodies, and Behavior in the Earlier Upper Paleolithic. Oxford University Press, Oxford.

Will, M., Stock, J.T., 2015. Spatial and temporal variation of body size among early *Homo*. J. Hum. Evol. 82, 15–33.